Ewais, A.M.R., Rowe, R.K., Rimal, S. and Sangam, H.P. (2018) "17-year elevated temperature study of HDPE geomembrane longevity in air, water and leachate", *Geosynthetics International*, 25(5), 525-544. https://doi.org/10.1680/jgein.18.00016

17-year elevated temperature study of HDPE geomembrane longevity in air, water and leachate

A.M.R. Ewais[1], R. Kerry Rowe[2*], S. Rimal[3] and H.P. Sangam[4]

[*]Corresponding author

[1] Assistant professor, Civil Engineering Department, Ain-Shams University, Cairo, Egypt, Email: amr.ragab@eng.asu.edu.eg, phone: +201067055740

[2] Professor, Canada Research Chair in Geotechnical and Geoenvironmental Engineering, and Killam Fellow, GeoEngineering Centre at Queen's-RMC, Queen's University, Ellis Hall, Kingston Ontario, Canada, K7L 3N6. E-mail: kerry@civil.queensu.ca, Phone: (613) 533-3113. Fax: (613) 533-2128.

[3] Geotechnical Engineer, Golder Associates Ltd., 6925 Century Avenue, Suite #100, Mississauga, Ontario, Canada L5N 7K2, E-mail: Santosh_Rimal@golder.com, Phone: +1 (905) 567 6100 Ext. 1232; Fax: +1 (905) 567 6561

[4] Director, Mine Environment, Mining & Metallurgy, SNC-Lavalin 195 The West Mall, Toronto | Ontario | Canada | M9C 5K1, Henri.Sangam@snclavalin.com, Phone: +1(416)679-6055, Fax: 1(416) 231-5336

Abstract

The results of 17-year investigation of a geomembrane (GMB) aged at 55, 70 and 85ºC in air, water and leachate are reported. At test termination, the mechanical properties had only reached nominal failure in leachate and water at 70 and 85ºC. Consistent with a previous study, there is a significant reduction in stress crack resistance (SCR) before there is clear evidence of oxidative degradation; this is attributed to the morphological changes due to disentanglement of entangled polymer chains. The effect of this apparent morphological change on SCR appeared to be greatest for the GMB when immersed in water and leachate at 70ºC, although it is evident for all fluids at all three test temperatures. Using the most conservative estimates, the time to nominal failure (t_{NF}, time to 50% of the initial or specified property value) in leachate, water and air (no UV exposure) ranged from >13, 18 and 170 years at 60ºC to 660, 1500, and 1700 years, respectively, at 20ºC. Assuming negligible tensile strains in the GMB, the time to nominal failure of this GMB in a composite liner is likely estimated to vary from >50 years at 60ºC to >550 years at 35ºC and > 1100 years at 20ºC.

Keywords: Geosynthetics, geomembrane, HDPE, degradation, service-life, landfill liner, chain disentanglement.

1. Introduction

High density polyethylene (HDPE) geomembranes (GMBs) are used as component of engineered barriers at municipal solid waste (MSW) landfills and many other types of landfills (e.g., hazardous waste, ash, for blast furnace slag, low level radioactive waste, etc.) to control the escape of leachate and gases from these facilities to the surrounding environment to a negligible level. They may be used in landfill covers/caps (Gallagher et al. 2016), base liners (Rowe 2005, 2012), and leachate lagoons (Rowe et al. 2003; Gassner 2017).

When used as part of a composite liner at the base of landfills, the geomembrane temperature may range from about the annual average ambient which is 10-20^{o}C in many parts of the world (e.g., in a low level nuclear waste containment mound), to 30-40^{o}C (e.g., in many MSW landfills in the methanogenic stage of degradation; Rowe 2012), to 60^{o}C in some MSW landfills (e.g., some bioreactors; Rowe 2012) and to 85^{o}C in unusual MSW landfills (Rowe 2012, Stark et al. 2012; Benson 2017; Reinhart et al. 2017; Stark and Jafari 2017).

With time, HDPE GMBs experience a reduction in their mechanical properties with increasing temperatures due to a change in the morphological structure of the GMB (Ewais and Rowe 2014a&b) and oxidative degradation (Hsuan and Koerner 1998; Müller and Jacob 2003; Müller et al. 2007). Thus, there is a need to understand the degradation of the GMB in exposure conditions similar to that in the field to interpret the GMB long-term performance. The longer the monitoring period, the better interpretation for the long-term performance of the GMB (Rowe and Ewais 2014).

The common chemical degradation model for HDPE GMBs conceptually involves three distinct stages (Viebke et al. 1994; Hsuan and Koerner 1998): (a) Stage I: characterized by the depletion of active antioxidants/stabilizers, (b) Stage II: an induction period, starting after Stage I, in which the geomembrane degrades without a measurable change in its engineering properties and (c) Stage III: characterized by a measurable change in the engineering properties of the

geomembrane (end of Stage II) due to degradation of the polymer that eventually leads to nominal failure (i.e., a drop to 50% of the initial or specified value). However GMB degradation trend does not always follow the conceptual model. For example, GMB may experience a loss in its SCR shortly after the ageing starts due to morphological change without other evidence of chemical degradation (Ewais and Rowe 2014a). However, it can also occur that a GMB may undergo thermo-oxidative degradation of its physical properties despite a high value of HP-OIT, suggesting that the antioxidants–stabilizers measured by the HP-OIT were not protecting the GMB (Ewais et al. 2014a; Ewais and Rowe 2014b).

A geomembrane may be considered to have reached the end of its service-life and have failed when it no longer meets the original design requirements as a hydraulic and diffusive barrier to contaminant migration (Rowe et al. 2004). In laboratory accelerated ageing immersion tests, there is no external stress applied to the geomembrane and it would not be expected to rupture. Thus, the end of Stage III is defined in terms of nominal failure which may correspond to the time at which a property of interest has decreased to 50% of either (a) its initial value (Hsuan and Koerner 1998) or (b) the value specified (e.g., by GRI-GM13) (Rowe et al. 2009). The latter approach takes into account the fact that some manufacturers provide products which far exceed the requirements of the specification (e.g., geomembranes with high initial SCR).

Rowe and Rimal (2008) and Rowe et al. (2010) aged an HDPE GMB in a composite liner configuration and their findings showed that the antioxidant depletion time of GMB aged in composite liner configuration were greater than that estimated for GMB aged in leachate immersion because GMB in leachate immersion was exposed to leachate from both sides; whereas, in a landfill composite liner, a GMB would be exposed to leachate at its top surface only and unsaturated (typically nearly saturated) geosynthetic clay liner or compacted clay liner at its bottom surface (Sangam and Rowe, 2002; Rowe et al. 2009). The greater the exposure to leachate, the more accelerated the depletion of antioxidants from the GMB because leachate has

surfactant and trace metals that would accelerate the depletion of antioxidants from the GMB (Myers 1988; Osawa, 1992; Rowe et al. 2008). Sangam and Rowe (2002) proposed simplified approach to infer the service-life (time to failure) of a GMB in composite liner configuration ($t_{f(comp)}$) based on immersion tests (GMB exposed to the same fluid from both sides) in air, water and leachate; viz.:

$$t_{NF\ (comp)} = 0.5^{*}\ (t_{NF(leachate)} + t_{NF(unsat)}) \quad (1)$$

$$t_{NF\ (unsat)} = 0.5^{*}\ (t_{NF(air)} + t_{NFwater)}) \quad (2)$$

where: $t_{NF\ (leachate)}$, $t_{NF\ (air)}$ and $t_{NF\ (water)}$ are the times to nominal failure of a GMB) in leachate, air and water exposures, respectively.

This simplified approach does not explicitly consider the effect of strains/stresses induced in the GMB in composite liner. These strains may arise from composite liner interaction involving: (a) local indentations of GMBs induced by the overlying drainage materials and by gravel in the underlying clay liner, and (b) down-drag load for GMBs on side slopes generated by waste settlement. The local strains associated with the indentations of the GMB liners caused by overlying granular drainage layer with and without a protection layer has been extensively examined (e.g., Brachman and Gudina 2008a, 2008b; Dickinson and Brachman 2008; Brachman and Sabir 2010, 2013; Hornsey and Wishaw 2012; Sabir and Brachman 2012; Rowe et al. 2013; Eldesouky and Brachman 2017). Also important, but having received less attention, are the strains induced by granular particles in the underlying compacted clay liner (Brachman and Sabir 2010). Another important potential source of tensile strain is that induced on side slopes due to waste weight, settlement, and degradation (e.g., Jones and Dixon 2005; Thusyanthan et al. 2007; Fowmes 2007; Fowmes et al. 2008a,b; Arab 2011; Sia and Dixon 2012; Wu 2013; Zamara et al. 2014; Kavazanjian and Gutierrez 2017; Yu and Rowe 2018a, 2018b; Kavazanjian et al. 2018). Construction related factors that can contribute to tensile strains in the geomembrane include

wrinkles that are locked into the geomembrane when it is covered (e.g., Gudina and Brachman, 2006; Brachman and Gudina 2008b; Rowe et al. 2012; Take et al. 2012; Yang et al. 2017) and welds (Giroud et al. 1995; Kavazanjian et al. 2017).

The importance of tensile strains in a liner was illustrated by Abdelaal et al. (2014) and Ewais et al. (2014b) who demonstrated that that tensile strain in excess of about 5% eventually will result in rupturing the GMB with the time to rupture being a function of the stress cracks resistance and the temperature. For example, Ewais et al. (2014b) reported that the equivalent of two million holes per hectare developed in a GMB aged in a composite liner configuration under applied pressure of 250 kPa (equivalent to the weight of approximately 15-25 m of waste, depending on density) in as little as three years at 85^{o}C because of the high strains/stresses developed in the GMB with an initial stress crack resistance (SCR) of about 900 hours due to composite liner interaction. The composite liner tested by Ewais et al. (2014a) comprised (from top to bottom) (a) poorly graded 50 mm crushed limestone (washed clear stone), (b) needle-punched nonwoven geotextile protection (cushion) layer with a mass per unit area of 580 g/m^2 (ASTM D5261), (c) a 1.5 mm thick HDPE GMB, and (d) a geosynthetic clay liner with a minimum bentonite mass per unit area of 3660 g/m^2.

The maximum allowable strain has yet to be determined, however it is known that cracking can occur at 6% tensile strain (Abdelaal et al. 2014) and later unpublished work has cracking at 4% tensile strain. Hence, based on this, the tensile strain should not exceed the 3% recommended by Seeger and Műller (2003). If the tensile strains are kept below the maximum allowable value, estimates of the service-life of GMB in landfill composite liner using the simplified approach (Equation 2) is considered to provide insight into the actual service-life in the field.

This paper reports the latest findings of a seventeen years investigation into the degradation in the properties of a nominally HDPE GMB aged in air, water and leachate. The

investigation started in air and water in 1997 and in leachate in 1999. The first results of this investigation were reported by Sangam and Rowe (2002) while Rowe et al. (2009) provided a detailed investigation and predictions for Stage I after monitoring the depletion of antioxidants for 8 to 10 years. Thus, the focus of this investigation is on interpreting the degradation Stages II and III in air, water and leachate at three different temperature (i.e., 55, 70 and 85^{o}C) based on the changes in SCR, MI and tensile properties over an additional 7.3 years. It will be the last such report since all the GMB coupons have now been tested. The total investigation period reported in this study is the longest investigation reported to date for accelerated immersion testing for a GMB. The monitoring period reported herein at 55^{o}C is 204 months (17 years) in air and water, and 181 months (15 years) in simulated MSW leachate (Figure 1).

The primary objective of this paper is to provide predictions for Stages II + Stage III and times to nominal failure for the GMB after up to 17 years of monitoring the GMB's degradation in air, water and leachate. The secondary objective is to use the estimated times to nominal failure in air, water and leachate to provide insight for the service-life of the GMB in composite liner configuration using Sangam and Rowe (2002) approach described above. Although the GMB examined herein was manufactured in 1997, its crystallinity and stress crack resistance are closer to those measured for "HDPE" GMBs manufactured since 2010 than the typical HDPE GMB properties manufactured in 1997.

2. Material and Ageing Conditions

The GMB with properties listed in Table 1 was manufactured by GSE Linings Inc. (although it is thought to have been manufactured using a flat die, possibly from a former Schlegel Lining Technology line after they joined with Gundle Lining Systems to form GSE in 1995). The geomembrane has a flow rate ratio of about 29 (suggesting a flat die resin). It had a reactively low (for HDPE in 1997) crystallinity of 44% (typically 59±4% around 1997 and earlier; modern HDPE is more typically 50±4%, and modern LLDPE typically 38±4% based on GMBs tested in

Queen's University's GMB laboratory). The GMB total density of 0.94 g/cm^3 classifies it as "HDPE" as defined by GRI-GM13 (2014) but it is at the top end of the medium density polyethylene (MDPE) range defined by ASTM D883 and very close to the HDPE lower limit (0.941 g/cm^3). Given the presence of 2.54% carbon black, the resin was almost certainly MDPE and this GMB may be regarded as somewhat of a pioneer of "HDPE" GMBs being produced today with MDPE resin and relatively high SCR.

The relatively low density may explain the relatively high initial stress crack resistance (SCR_o), obtained from the single point notched constant tensile load (SP-NCTL; ASTM D5397) test of about 5200 hours (Table 1) for this geomembrane. This is much higher than the typical SCR measured for geomembranes at the time of its production when GRI-GM13 only required 200 hours of SCR. The initial SCR test reported by Sangam and Rowe (2002) sought simply to confirm that it met the required 200 hours and was terminated at 210 hours. Subsequently, tests were performed to failure to obtain a mean SCR (at failure) of 5220 hours with a coefficient of variation of 3%. Lowering the density of the geomembrane resin to the range of MDPE, increases its resistance to slow crack growth (Scheirs 2009; Hsuan 2013), because of the increase in the probability of occurrence of the inter-lamellar connections (e.g., tie molecules, Huang and Brown 1991). Considering the properties listed in Table 1, the geomembrane meets the requirements specified by Ontario Regulation 232/98 of the Environmental Protection Act (MoE, 1998) and the current GRI-GM13 (2016) although it was manufactured twenty years ago.

The GMB was aged in air, distilled water (pH=~6), and reduced synthetic leachate at three different temperatures (55, 70 and 85^{o}C). The reduced leachate was prepared based on the analysis of the leachate from the Keele Valley MSW landfill (Hrapovic 2001) by mixing volatile fatty acids, inorganic salts, trace metals, and surfactant in water (the full chemistry is given by Sangam and Rowe 2002 and Rowe et al 2009). The effect of various constituents in leachate has been discussed by Abdelaal et al. (2014b) based on a nine (9) year ageing study of another GMB

in different simulated MSW leachates including the one examined herein. There was limited degradation of the physical properties reported by Rowe et al. (2009) at 85ºC in leachate and water. Also, it was recognized that at 55ºC the rate of degradation in air and water were remarkably slow (as confirmed by 17 years of monitoring, Figure 1). Thus, to improve the interpretation of Stage II and Stage III, some GMB coupons were moved from 55ºC air to 85ºC leachate and from 55ºC water to 85ºC water and the degradation of the GMB properties were monitored with time. After the GMB reached the end of Stage II at 85ºC, some coupons that were moved back from water and leachate to age in water and air, respectively, at 55ºC to monitor the degradation of the GMB during Stage III at 55ºC; hence, alternatively estimate Stage III at 55ºC in water and air exposures. Thus, at 55ºC in water and air, there were two sets of coupons such that one set was aged at 55ºC from beginning of ageing and the other set was aged at 55ºC after the end of Stage II.

Due to a paucity of coupons aged at 70ºC in any fluid after OIT depletion, jars of coupons that were ageing at 40ºC were moved to 70ºC ovens and the degradations in the physical properties were monitored with time to interpret Stage II and Stage III at 70ºC in air, water and leachate exposures.

3. Testing and Methods

The change in the stress crack resistance SCR; single point notched constant tensile load, SP-NCTL, as per ASTM D5397-appendix), melt index (MI; ASTM D1238), and tensile strength and elongation at break (ASTM D6693) of the GMB were monitored with time to investigate Stages II and III of the GMB. The SCR is the measure of the resistance of the GMB to slow crack growth under sustained stress (Hsuan et al. 1993a,b). The melt flow index is rough indicator of either an increase in molecular weight due to cross-linking or a decrease in molecular weight due to chain scission that may occur in aged polymeric geomembranes due to thermal or thermal-oxidative degradation (Shenoy and Saini 1986; Hsuan and Koerner 1998; Peacock 2000; Scheirs

2000). The melt indices of the aged samples were measured using a weight of 2.16 kg at 190°C. The tensile tests were conducted using Type IV specimens (ASTM D6693) at an elongation rate of 50 mm/minute and the strength and elongation at break were recorded with ageing time.

4. Results and Discussion

Rowe et al. (2009) provided predictions for length of Stage I (Δt_I) for different temperatures and exposure conditions based on 8-10 years of data (Table 2). The focus here is on interpreting length of Stage II (Δt_{II}) and Stage III (Δt_{II}) in air, water, and leachate based on changes in SCR and tensile break properties at 55, 70 and 85°C. The time to nominal failure, ($t_{NF} = \Delta t_I + \Delta t_{II} + \Delta t_{III}$) are estimated for the GMB based on SCR and tensile break properties (Table 2) as they are more representative for the geomembrane resistance to the applied load in the field than MI which, while a useful indicator for degradation in the GMB, is not directly related to the field performance

For the GMB examined, the traditional definition of t_{NF} equal to the half-life of GMB property examined was used for the tensile properties as will be discussed. But the definition of the nominal failure, and hence, t_{NF}, based on SCR was challenging because of: (a) the very high initial SCR_o (5220 ± 160 hours) of the GMB, and (b) the change in the requirements for SCR by GRI-GM13 over the years from SCR_{req} = 200 hours in 1997, to 300 hours in May 2003, and 500 hours in November 2014. Thus, SCR at nominal failure based on traditional definition (SCR_{NF}) would be ~2610 hours (more than five times the initial value presently required by GRI-GM13 and 13 times that required in 1997). Thus, it was considered to make more sense to use SCR_{NF} = 0.5 SCR_{req}, but which value? Since 300 hours was the requirement for the longest period and is an intermediate value, it was selected in this paper as the basis for SCR_{NF} = 0.5 SCR_{req} = 150 hours.

Ewais and Rowe (2014 a & b) observed that during Stage I and Stage II there may be a drop/change in stress crack resistance (SCR) and tensile break properties due to morphological change rather than degradation of the polymer, especially at the temperatures considered in this

paper. The morphological change may arise from two mechanisms that can affect SCR, namely: annealing and physical chain disentanglement. Annealing can increase the strength of the inter-lamellar connections thereby increasing the SCR. Chain disentanglement would decrease the number of the inter-lamellar connections thereby decreasing SCR. The magnitude of morphological changes due to either the chain disentanglement and/or annealing would depend on incubation conditions as well as the thermal and stress history experienced by the GMB during manufacturing (Ewais and Rowe 2014c). The thermal and stress histories also would affect the orientation of the crystal lamella affecting the SCR of the GMB (Ewais and Rowe 2014a). Thus, if different locations within the GMB experienced different thermal and stress histories during manufacture the effect of morphological changes on the SCR would vary within the same GMB resulting in a variability (fluctuation) in the measured SCR; the wide range of SCR observed for this GMB with the same length of aging may, at least in part, be due to different thermal and stress histories at different locations in the roll and/or the effect carbon black distribution in the amorphous zone which could affect chain entanglement and SCR. This is likely one of the factors contributing to the variability in stress crack resistance as discussed by Ramsey et al. (2018) and reported by the Geosynthetic Accreditation Institute – Laboratory Accreditation Program (GAI-LAP) which listed the uncertainty of the measured SCR test as much as 21% (Koerner, 2016).

In this study, estimating the length of the Stage II (Δt_{II}) was challenging because: (a) there was fluctuation in SCR measured with ageing, and (b) when there was a drop in mechanical properties, it was not always clear if the drop was due to morphological change, chemical degradation or, possibly, a little of both. Given the uncertainty and the consequent range of plausible interpretations that can be used to estimate the Δt_{II} and length of Stage III (Δt_{III}), when this uncertainty arose, two approaches were followed for fitting the data. In Approach A, morphological change was considered to be the main cause of the drop in SCR, tensile break elongation (TBE) and break strength (TBS) of the GMB with little contribution from chemical

degradation. In Approach B, chemical degradation was also considered to contribute to the drop in SCR, TBE and TBS as manifested by the changes in melt index (MI), when applicable. Because morphological degradation and the chemical degradation are difficult to distinguish from each other based on the current knowledge (Ewais and Rowe 2014a), different plausible interpretations of the data can give different Δt_{II} and Δt_{III} when Approach B is applicable. Where both approaches were followed it is considered reasonably likely that in fact there is little or no chemical degradation and that the change is morphological (i.e., that Approach A is reasonably likely). However, to be conservative, for the purposes of estimating Δt_{II} and Δt_{III}, Approach B was adopted for the Arrhenius modelling. Thus the estimated times to nominal failure are considered conservative and they may be very conservative. Despite this conservative approach, as discussed below, the degradation of the GMB was remarkably slow and the estimated t_{NF} are remarkably long. Also, since the end of Stage I and Stage III are far better defined than the transition from Stage II to III, there is far less uncertainly regrading $\Delta t_{II} + \Delta t_{III}$ than the individual components Δt_{II} and Δt_{III}, and hence $t_{NF} = \Delta t_I + \Delta t_{II} + \Delta t_{III}$ is not sensitive to the uncertainly regrading $\Delta t_{II} + \Delta t_{III}$. For example, the application of Approaches "A & B" in interpreting Δt_{II} and Δt_{III} for SCR, TBE and TBS data for GMB samples aged in air at 85ºC (Figure 2) is discussed in the following paragraphs. In the following times are usually reported as "after the end of Stage I" and these times are designated by "I+" meaning the time elapsed following Stage I.

Over the 65 months (5.3 years, Figure 2) in air at 85ºC following Stage I, the GMB experienced a drop in both TBS and TBE to about 70% of the initial value. It could be argued that this drop was due to morphological change since after I+65 (with a little scatter) the TBE and TBS data remained constant until the end of monitoring (the horizontal line marked as "Approach A" in Figure 2b) implying with no oxidative degradation during this 85 month period. In this interpretation, the GMB was still in Stage II for at least 150 months past Stage I. Similarly, over the same period of time (I+65 months), the mean SCR also appears to have decreased to about

20% of the initial value (average mean value of ~ 1050 hours with a range of fluctuation in mean values from 850 to 1500 hours) and remained essentially constant (horizontal line "Approach A" in Figure 2a) at this value for the remainder of the testing. Again this could be interpreted as a morphological drop with little oxidative degradation. Thus, there appears to be consistency between TBE, TBS and SCR data following Approach A, suggesting that the changes are due to morphological changes and not oxidative degradation and hence the GMB was still in Stage II 150 months past Stage I (i.e. $\Delta t_{II} > 150$ months). Since, following Approach A, Stage III had not yet started even after 17 years of testing at 85°, and Δt_{III} is unknown.

Despite the forgoing, the possibility of oxidative degradation cannot be excluded when the MI data (Figure 2a) are considered. The MI began to decrease between about 4 and 37 months after the end of Stage I (i.e., I+4 to I+37 months) and by I+65 months was very low (it could not be measured by I+77 months). This suggests (but does not prove) that degradation with cross-linking of the polymer chains began sometime around I+37 months and hence an alternative interpretation (shown by the solid decreasing lines labelled "Approach B" in Figure 2) gives the end of Stage II at about 37 months for SCR, TBE and TBS and a projected Δt_{III} of 113 (SCR), 193 (TBE) and 201 (TBS) months. This interpretation (Approach B) did not give much weight to the TBE and TBS data measured at I+65 and I+67 months, and resulted in projected value of SCR~150 hours at I+150 months although it was measured to be ~ 1200 hours (range of 1500 – 970 hours on replicate specimens states at same age) at I+150 months. Although the assumptions made following Approach B here are considered very conservative, they still result in remarkably very long values of Δt_{II} and Δt_{III} .

To investigate the effect of uncertainty in estimating end of Stage II (and hence the relative contribution of Δt_{II} and Δt_{III}) on t_{NF} estimated from Arrhenius modeling. t_{NF}, at any temperature of interest were obtained twice following two methods. The first method involved the summation of Δt_I, Δt_{II} and Δt_{III} after each value was estimated from the Arrhenius modeling for

Δt_I, Δt_{II} and Δt_{III}, respectively. The second method involved the summation of the values of Δt_I and $\Delta t_{II}+\Delta t_{III}$ that were estimated from Arrhenius modeling for Δt_I and $\Delta t_{II}+\Delta t_{III}$, respectively. By using the Arrhenius fits for $\Delta t_{II}+\Delta t_{III}$ (i.e., from the end of Stage I to end of Stage III), the uncertainty in determining the time of the end of Stage II was excluded and did not affect the estimated t_{NF}. It was found that the t_{NF} obtained using the two methods were only slightly different as will be discussed later in the paper. Thus, although a precise estimate of Δt_{II} and Δt_{III} is scientifically interesting, it did not greatly impact the estimated t_{NF}, implying that the uncertainty in estimating end of Stage II had minor impact on the t_{NF} estimated from Arrhenius modeling.

4.1. Degradation at 85ºC

For all exposure conditions at 85ºC, the measured MI fluctuated with time between 80 to 100% of the initial value before it started to decrease significantly with time to negligible values (Figure 2 to Figure 4). The significant decrease in MI is likely an indication of an increase in the molecular weight due to cross-linking during ageing (Shenoy and Saini 1986; Hsuan and Koerner 1998) resulting from thermo-oxidative degradation (Bolland and Gee 1946; Hawkins 1964; Winslow et al. 1966; Gugumus 2002) and/or thermal degradation in the absence of oxygen (Holström and Sörvik 1974; Kuroki et al. 1982).

In air at 85ºC, the MI reached negligible values (~ zero) while significant values for SCR, TBS and TBE were measured, implying that the MI may not be a good indicator for degradation in GMB mechanical properties in air. In water and leachate, the MI of GMB coupons had a half-life of about 2-3 months beyond Stage I. Negligible MI values were attained within the same time frame in which the SCR reached 150 hours in water (Figure 3a) however, in leachate, negligible values were reached about 4 months before SCR reached 150 hours (Figure 4a). Thus, MI data should be used with caution especially in evaluation of the GMB performance in the field.

Following Approach A for samples in air, t_{NF} is not known for SCR, TBS and TBE because the end of Stage II was not evident in 17 years of monitoring. However, this gives a lower bound on the possible value of $t_{NF} > \Delta t_I + \Delta t_{II} > 27+150=177$ months. Following Approach B, the t_{NF} ($\Delta t_I + \Delta t_{II} + \Delta t_{III}$) = (27+37+113) = 177 months based on SCR, are t_{NF} = (27+ 37+ 201) = 265 based on TBS and t_{NF} = (27+ 37+ 193) = 257 months for TBE (Table 2).

In water (Figure 3), SCR fluctuated varied between 0.55 and 0.08 SCR_o over the first 12 months of ageing beyond Stage I (I+12 months, Figure 3a). The SCR was 60 hours at I+13.4 months implying it reached nominal failure before I+13.4 months (Figure 3a). Approach A (assuming no chemical degradation took place) was not used in this case since it appeared the GMB reached nominal failure. Following Approach B (assuming the drop in SCR is due to both chemical degradation and morphological changes), there is uncertainty regarding the end of Stage II since the data may be fitted in different ways (e.g., the dashed and solid line fits in Figure 3a). The solid line was based on taking I to I+9 months as Stage II where morphological change was the dominant mechanism decreasing SCR (Figure 3a) and where chemical degradation was the dominant mechanism between I+9 to I+14 month such that in Stage III the three SCR data points between I+9 to I+14 months lie on a straight line (Figure 3a) giving $t_{NF} = \Delta t_I + (\Delta t_{II} + \Delta t_{III})$ = (24+9+3) = 36 months. An alternative interpretation (the dashed curve in Figure 3a) assumed that only the drop in the first two months was Stage II and that after I+2 months chemical degradation dominated resulting in $t_{NF} = \Delta t_I + \Delta t_{II} + \Delta t_{III}$ = (24+2+10) = 36 months. Although the two SCR fits gave the same t_{NF}, the lack of significant change in TBS and TBE over the first 10 months is more in agreement with the solid line fit of SCR as discussed in the following paragraph. Also a value of Δt_{III} = 10 months (the dashed fit) results in an unacceptable greater Δt_{III} than that estimated at 70°C as discussed below. Thus, based on the preponderance of evidence the solid line fit is considered most reasonable and the consequent values of Δt_{II} and Δt_{III} are given in Table 2 to be used later in the Arrhenius modelling.

The TBS and TBE fluctuated with ageing between 80 to 100% of the initial value (Figure 3b) until they started to significantly degrade (Δt_{II}) between 9 and 12 months after Stage I resulting in Δt_{III} of about 8 and 2 months, respectively, as interpreted from the lines fit following Approach B (Figure 3b). SCR (solid line fit), TBS and TBE data had a consistent degradation behaviour in which a fluctuation in the measured values up to 9-12 months in Stage II followed with significant drop in Stage III. This consistent degradation behaviour implies that the fluctuation in properties for the first 9-12 months is due to morphological changes with little to no chemical degradation. Following this reasoning, $t_{NF} = \Delta t_I+\Delta t_{II}+\Delta t_{III}$ = (24+9+8) = 42 months for TBS and t_{NF} = (24+12+2) = 38 months for TBE and these values (Table 2) will be used in the Arrhenius modelling.

Immersed in leachate (Figure 4), the mean SCR fluctuated between 0.43 SCR_o and 0.12 SCR_o during the first 11 months (to I+11 months, Figure 4a) with an average of 0.21 SCR_o (1100 hours). The SCR was 60 hours at I+29 months implying it reached nominal failure before I+29 months (Figure 4a). Two fits to the data were considered (Figure 4a). The solid line fit assumed morphological change was the dominating mechanism for the first 9 months (Δt_{II} =9 months) and that chemical degradation dominated between 9 to 11 months (Figure 3a) with a straight line fit resulting in $t_{NF} = \Delta t_I+\Delta t_{II}+\Delta t_{III}$ = 10+9+3 = 22 months (Figure 3a). Alternatively, the dashed curve fit (Figure 4a) is based on the observation that the MI data decreased significantly after I+ 2 months and assumes that this was due to chemical degradation, therefore giving Δt_{II} =2 months and $t_{NF} = \Delta t_I+\Delta t_{II}+\Delta t_{III}$ = 10 + 2 + 14 = 26 months. However, considering that the MI data has dropped to 50% of the initial value in 3 months and reached negligible values in 7 months beyond Stage I it appears that the dashed curve fit for SCR maybe a little optimistic (Figure 4a). Thus, t_{NF}, Δt_{II} and Δt_{III} for SCR estimated from solid line fit (Table 2) were used (conservatively) in the Arrhenius modelling.

The TBS and TBE fluctuated with ageing between 80 to 100% of the initial value (Figure 3b) until they started to significantly degrade giving Δt_{II} of about 18 months and based on a straight line fit to the subsequent Stage III data gave Δt_{III} of about 11 months for TBS and 8 months for TBE following Approach B (Figure 3b). Thus, at 85ºC in leachate, $t_{NF} = \Delta t_I + \Delta t_{II} + \Delta t_{III}$ = 10+9+3 = 22 months for SCR, t_{NF} = 10+ 18+ 11 = 39 months for TBS, and t_{NF} = 10+18+8 = 36 months based on TBE (Table 2).

4.2 Degradation of the geomembrane at 70ºC

Over the 70 months of monitoring beyond Stage I in air (Figure 5), the MI fluctuated between 80 and 100% of the initial value but no significant degradation in the MI was observed (Figure 5a). The mean SCR fluctuated between 0.86 SCR_o (4510 hours) and 0.09 SCR_o (465 hours). The fluctuation did not follow an obvious pattern for example it fluctuated initially around 0.86 SCR_o first 5 months beyond Stage I and then it appeared to drop rapidly to about 0.09 SCR_o (about 470 hours) at I+8 months but with ageing the measured SCR significantly increased reaching in some occasions 0.86 SCR_o over the remainder of the 70 months of monitoring. Although the reason of such fluctuation in SCR is uncertain, it may be due to non-uniform morphological changes in the GMB. This non-uniform changes may be due to: (a) the GMB initially experience physical chain disentanglement resulting in decreasing its SCR, but with ageing, the crystal lamella of the GMB may undergo annealing which increased the strength of the inter-lamellar connections and in turn increased the SCR of the GMB; and/or (b) the GMB experienced different thermal histories at different locations during the manufacturing process resulting in different SCR of the GMB when measured at these location. Ewais and Rowe (2014c) highlighted the significant effect of thermal and stresses histories on the SCR of GMB when examined geomembranes with different thicknesses manufactured at the same production run from the same resin.

The SCR did not reach nominal failure during the 70 months beyond Stage I (consistent with the Approach A interpretation that it was not reached at 85ºC). The TBE and TBS (Figure

5b) fluctuated at around 90 and 100% during the entire post Stage I monitoring period with no evidenced of oxidative degradation. Thus, as was the case at 85ºC, it was not possible to estimate Δt_{II} and Δt_{III}, although Δt_{II} exceeds 70 months post Stage I and it can be inferred that t_{NF} exceeds the values (conservatively) inferred for 85ºC (Table 2).

In water (Figure 6), the MI remained at about the initial value from I+6 to I+10 months and then decreased at a relatively consistent rate reaching 50% of the initial value at about I+24 and negligible value at about I+44 months. The mean SCR fluctuated between 0.42 SCR_o (2220 hours) and 0.09 SCR_o (491 hours) with a mean of 0.2 SCR_o (1050 Hours) until about I+33 months (Figure 6a). The mean SCR was 186 (range 45 to 320) hours at I+37 and 73 hours at I+49 months, implying it reached nominal failure at about I+37 months (Figure 6a). Approach A was not used as it appeared the GMB reached nominal failure. Adopting Approach B, the solid line fit (Figure 6a) resulted in Δt_{II} of about 30 and Δt_{III} of 7 months. The TBE and TBS fluctuated above 85% of the initial values until they started to significantly degrade reaching 50% of the initial values (Figure 6b). Following Approach B, two fits were attempted for each tensile property resulting in the same t_{NF} such that $46 \leq \Delta t_{II} \leq 50$ months and $11 \geq \Delta t_{III} \geq 7$ months for TBE and $42 \leq \Delta t_{II} \leq 46$ and $15 \geq \Delta t_{III} \geq 11$ months for TBS. Taking the lower value for Δt_{III} will result in little difference to that estimated at 85ºC in water which does not seem reasonable since higher degradation is expected at higher temperature. Thus, the upper conservative limit of the estimated Δt_{III} were considered to be more reasonable values such that $t_{NF} = \Delta t_I + \Delta t_{II} + \Delta t_{III} = 38+30+7 = 75$ months, $t_{NF} = 38+42+15 = 95$ months, and $t_{NF} = 38+46+11 = 95$ months based on SCR, TBS and TBE respectively (Table 2).

In leachate (Figure 7), the MI remained relatively constant at the initial value until about I+15 months and then decreased at a relatively consistent rate reaching 50% of the initial value at about I+23 and negligible value at about I+30 months (Figure 7a). The mean SCR fluctuated between 0.42 SCR_o (2150 hours) and 0.05 (221 hours) until about I+31 months (Figure 7a) with

an average of 0.2 SCR_o (1100 hours). At I+37.6 months, the mean SCR was 72 (range 65 to 80) hours implying nominal failure had been reached just before I+37) months (Figure 7a). Approach B was followed as indicated by the solid line (Figure 7a) resulting in Δt_{II} of about 30 months and Δt_{III} of 7 months. TBE and TBS fluctuated above 85% of the initial values until about I+30 months and then started to significantly degrade reaching nominal failure (50% of the initial values, Figure 7b) at about I+43 (TBE) and I+59 (TBS) months. The interpreted Δt_{II} was about 30 months for both TBS and TBE; whereas, Δt_{III} was 29 months for TBS and 13 months for TBE. The corresponding values of t_{NF} were 54, 50 and 76 months for SCR, TBS and TBS respectively (Table 2).

4.3. Degradation of the geomembrane at 55ºC

Although the GMB samples were aged at 55ºC in air for around 204 months (Figure 1a), Stage I took 194 months (Table 2) and hence the GMB samples were only aged for 10 months beyond Stage I. This was not sufficient to observe measurable degradation in the GMB properties due to oxidative degradation and hence it was not possible to estimate the length Stages II for the samples aged from the initial (unaged) state. To provide some insight into the length of Stages II in air, a stage-parallel approach was adopted. This involved moving some GMB samples from air at 55ºC to 85ºC, ageing them in leachate for ~6 months to the end of Stage I, and then moving them back to 55ºC in air to monitor their degradation in air for 65 months. During ageing of the accelerated samples at 55ºC in air there was a drop in SCR to about 0.66 SCR_o but with very large range of test values (Figure 8) and this continued up to about I+6 after which SCR fluctuated between of 0.5 SCR_o and 0.25 SCR_o with an average value of 0.35 SCR_o. Since there was no measurable decrease in the MI, TBS or TBE during the accelerated ageing or over the subsequent 65 months (Figure 8) and SCR also stabilized, the change in SCR was attributed to morphological change and it was inferred that the samples were in Stage II for the full 65 months of post Stage I monitoring. This indicates that Δt_{II} exceeds 65 months at 55ºC and since it is known to exceed 70

months at 70ºC (as discussed above), it can be inferred that Δt_{II} >> 70 months while Δt_{III} remains unknown. Since the t_{NF} at 55ºC is expected to be much longer than that at 85ºC, it is inferred that it must be much greater than that t_{NF} >> 177, 257 and 265 months for SCR, TBE and TBS respectively (Table 2).

In leachate at 55ºC (Figure 9), MI fluctuated between 0.78 and 1.0 MI_o but there was no consistent decrease in the MI over the period monitored (to I+152 months). Similarly, TBE and TBS fluctuated between 0.85 and 1.05 of the initial value with no consistent decrease. The mean SCR fluctuated between 0.6 (3120 hours) SCR_o and 0.3 SCR_o (1580 hours) and stabilized at around 0.44 SCR_o (2330 hours) with no clear evidence of a decrease other than due to morphological change. Based on this interpretation implying no oxidative degradation took place and Approach A (Figure 9b) Δt_{II} > 152 months and Δt_{III} is unknown. Adopting the alternative Approach B, based on a linear extrapolation through the last two data points (Figure 9a), Δt_{II} and Δt_{III} were estimated to be Δt_{II} = 143 months and Δt_{III} =108 months for SCR. Similarly, Δt_{II} =104 months and Δt_{III} =164 months for TBE, and Δt_{II} =104 months and Δt_{III} = 158 months for TBS.

In water (Figure 10), although the GMB samples were aged at 55ºC for around 204 months (Figure 1b). Stage I took 118 months (Table 2) and so the GMB samples were only aged for 86 months beyond Stage I (Figure 10). There was no measurable degradation in the MI and TBE or TBS (Figure 1b and Figure 10) during this period (i.e., no evidence of oxidative degradation). The average SCR fluctuated between 0.68 SCR_o (3520 hours) and 0.32 SCR_o (1674 hours; Figure 9a), due to morphological changes. Thus, it was not possible to determine the length of Stage II from these samples although it is known that Δt_{II} > 86 months for SCR, TBE and TBS.

Similar to air, the stage-parallel approach was adopted to monitor Stage III by moving coupons from water at 55ºC to 85ºC to what was thought to be the end of Stage II and moved back to 55ºC in water where they were monitored for 60 months (Figure 11). After moving the

coupons to 55ºC in water, there was no measurable decrease in the MI or tensile break strength and elongation (Figure 11). The SCR fluctuations (Figure 10a) were similar to that of the samples aged from the beginning to the end at 55ºC in water (Figure 9a) implying no degradation in the SCR due to oxidative degradation such that the SCR stabilized at a value of 0.35 SCR_o (Approach A, Figure 10a). Following Approach A, it was not possible to estimate Δt_{III} since, based on this interpretation, the coupons were still in Stage II and it is known from Figure 9 that known that $\Delta t_{II} > 86$. The alternative Approach B when interpreting the fluctuation in the SCR data from of the stage-parallel samples (Figure 11a) results in an estimate of $\Delta t_{II} = 108$ months (Table 2).

Based on the conservative inference for leachate (Approach B) for SCR it is possible to improve the estimate for Stage III for water at 55ºC since it is known from other results presented here that the interpreted Δt_{II} and Δt_{III} for SCR in leachate and water were the same at 70ºC (30 and 7 months) and 85^{oC} (3 and 9 months). Similarly, the interpreted Δt_{III} at 55ºC in water and leachate were equal 108 months. Thus, Δt_{II} in water at 55ºC is assumed equal to that conservatively estimated in leachate (143 months, Table 2) taking into consideration that Δt_{II} in water at 55ºC is know to be > 86 months (Figure 10a) based on SCR data (Table 2).

4.4. Drop in SCR with ageing

As discussed earlier in all exposures and temperatures, the SCR fluctuated significantly until either reaching nominal failure or the end of the monitoring period. This fluctuation is inferred to be due to non-uniform rate of disentanglement of the physical chain in the amorphous zone of the GMB (Ewais and Rowe 2014a). Plotting the mean of the fluctuation at all incubations temperatures (the error bars represent the minimum and maximum mean values), it was observed (Figure 12) that: (i) the fluctuation in water and leachate were less (statistically significant at the 95% confidence level) than that in air, (ii) while there was very little (not statistically significant) difference between the mean values in water and leachate, the mean value in air was consistently

higher than both (although, given the magnitude of the variability the difference is not statistically significant), and (iii) at 70ºC the mean SCR reached lower values than that were observed at 55 and 85ºC. The first two observations are consistent with the suggestion by Ewais and Rowe (2014a) that the lubrication of the chain in the amorphous zone by the diffusion of water and surfactant molecules in the leachate may facilitate the disentanglement of the physical chain entanglements better than in air. The third observation implies that the disentanglement was greater at 70ºC than at 85 and 55ºC, although the variability at all temperatures is such that the differences, although apparent in terms of the mean value, are not statistically significant. That said, the latter observation is different to that of Ewais and Rowe (2014a) who observed greater disentanglements of physical chain entanglements at 55ºC. If the difference is real, this would imply that the temperature at which the greater disentanglement may occur differs from GMB to GMB; more research is needed to resolve this issue.

4.5. Prediction of times to nominal failure, t_{NF}

The predictions for Δt_I used to estimate the times to nominal failure listed in Tables 3 to 5 were based on Arrhenius modelling reported by Rowe et al. (2009) for the antioxidants depletion rates after 8-10 years of monitoring the depletion of the antioxidant from the investigated GMB. The estimated Δt_{II} and Δt_{III} at different temperatures (Table 2) were used to estimate the $\eta = 1/\Delta t_{II}$ and $\gamma = 1/\Delta t_{III}$ which are the degradation rates of the GMB property of interest during Stage II and Stage III respectively. Δt_{II} and Δt_{III} were estimated based on the change in SCR in water were equal to that in leachate (Table 2), thus, there was only one Arrhenius plot based for SCR for the degradation rates in water and leachate. In contrast, the Arrhenius plots based on tensile break properties in leachate (Figure 14) were different to those in water (Figure 15).

The Arrhenius equation used in Figure 13 to Figure 15 followed a relationship used by Koerner et al. (1992), viz:

$$s = A\, e^{-\left(E_a/RT\right)} \tag{3}$$

where: E_a is the activation energy (J.mol^{-1}) required by the reactants to react, R = universal gas constant (8.314 J.mol^{-1}.K^{-1}), T = absolute temperature in Kelvin (K), A is a constant and s is the degradation rate in months^{-1}. The Arrhenius equation (Eq. 3) can be rewritten for η, viz:

$$\ln(\eta) = \ln(A) - \left(E_a/RT\right) \tag{4}$$

and for γ, viz:

$$\ln(\gamma) = \ln(A) - \left(E_a/RT\right) \tag{5}$$

The equations used in the Arrhenius modelling for $\eta = 1/\Delta t_{II}$ and $\gamma = 1/\Delta t_{III}$ based on SCR, break elongation and break strength are presented in Figure 13, Figure 14 and Figure 15, respectively. Δt_{II} and Δt_{III} were estimated from these Arrhenius equations and, based on the summation of Δt_I, Δt_{II} and Δt_{III}, t_{NF} was calculated for immersion in leachate (Table 3) and water (Table 4) at range of temperatures (20-60°C). Table 6 compares the observed and predicted times to nominal failure in leachate and water at the three test temperatures. With a few exceptions, it can be seen that the predictions are generally consistent with the observed values.

As previously indicated, the significant fluctuations in SCR before reaching nominal failure (i.e., 150 hours) added some uncertainty in estimating the exact length of Stages II and III based on SCR. An alternative means of estimating t_{NF} involves using one degradation rate from the beginning of Stage II to the end of Stage III ($\Delta t_{II} + \Delta t_{III}$), instead of considering two degradation rates (i.e., η and γ) based on Δt_{II} and Δt_{III}, such that and $\delta = 1/(\Delta t_{II} + \Delta t_{III})$ is reciprocal of the time from the end of Stage I (which is well defined) and the end of Stage III (t_{NF}) which is also well defined. The Arrhenius equation (Equation 3 and Figure 13) can be rewritten for δ, viz:

$$\ln(\delta) = \ln(A) - \left(E_a/RT\right) \tag{6}$$

The times from the end of Stage I to the end of Stage III ($\Delta t_{II} + \Delta t_{III}$) at different temperatures (20-60°C) were estimated from this Arrhenius equation at different temperatures (20-60°C) as

presented in Table 3 and Table 4 for water and leachate, respectively. From 40 to 60ºC in either leachate and water, the predicted times from end of Stage I to end of Stage III ($\Delta t_{II} + \Delta t_{III}$) using the Arrhenius plot for the degradation rate δ were very close to that predicted using the Arrhenius plots of η and γ such that the rounded t_{NF} differed by less a year. Between 20 to 35ºC the difference increased with the use of the Arrhenius plot for δ to obtain the (rounded) t_{NF} being conservative by between 12% (at 20ºC) and 5% (at 35ºC) compared to that predicted adding 1/η and 1/γ for Stage II and Stage III separately. Thus, the uncertainty regarding when Stage II ended and Stage III began had only minor effect on the predicted t_{NF} and the use of the Arrhenius plot for δ was conservative.

Using the most conservative estimates based on SCR the times to nominal failure increased from ≥ 13 years at 60ºC to ≥ 1500 years at 20ºC in leachate and from ≥ 18 years at 60ºC to ≥ 1500 years at 20ºC in water (Table 2). Based on tensile break strength, the time to nominal failure increased from ≥ 16 at 60ºC to ≥ 660 years at 20ºC in leachate and from ≥ 20 years at 60ºC to ≥ 1700 years at 20ºC in water (Table 2). Similarly, based on tensile break elongation, the time to nominal failure increased from ≥ 14 at 60ºC to ≥ 900 years at 20ºC in leachate and from ≥ 21 years at 60ºC to ≥ 1700 years at 20ºC in water.

At air, despite 17 years of testing and using the stage-parallel method to help acceleration the generation of results it was only at 85ºC that it was possible to conservatively estimate: (a) the time from end of Stage I to end of Stage III based on SCR, and (b) Stage II and Stage III based on the tensile break elongation and strength. Thus, it was only possible to estimate δ based on SCR and, γ and η based on tensile break properties at one temperature (85ºC) and hence it was not possible to develop an Arrhenius plot for δ, γ and η in air. Following the approach used by Rowe et al. (2009), since δ, γ and η can be evaluated at 85ºC, therefore, they can be evaluated at any temperature using the following equation:

$$\frac{s_{85}}{s_T} = \exp\left(\frac{E_a}{R}\left(\frac{1}{T_{85}} - \frac{1}{T}\right)\right) \quad (7)$$

where: s_{85} is the degradation rate (i.e., δ, γ and η) estimated at 85ºC, s_T is the degradation rate at temperature of interest (T). Because it was not possible to estimate E_a/R in air for any property of interest, the values for E_a/R estimated in leachate based on SCR and tensile break properties were (conservatively) used in Equation (7) to predict the degradation rates based on SCR and tensile break properties in air at any temperature of interest; and hence, evaluate the degradation at Stage II and Stage III as presented in Table 5. Following this approach, the times to nominal failure in air increased from: 170 to > 1700 years (capping higher predictions above 1700 years at 1700 years; actual predicted value was an order of magnitude higher) based on SCR, 220 to 1700 years based on tensile break elongation, and, 170 to 1700 years based on tensile break strength (Table 5).

4.6. Prediction of GMB service-life in landfill composite liner

Following Sangam and Rowe (2002) simplified approach (Equation 2) to infer the GMB service-life in composite liner configuration (Table 7), the time to nominal failure for this GMB in a composite liner configuration was calculated based on both the SCR, TBE and TBS and also the minimums values of t_{NF} given in Tables 3-5. Based on the conservative interpretations adopted, t_{NF} would likely increase from >54 years at 60ºC to more than >1100 years at 20ºC. It should be acknowledged that these values are estimated based on degradation of the GMB properties under no stresses and assume that the design is such that the strains are kept to below about 3%, and certainly less than 5%, based on available information. The interpretation, herein, were conservatively estimated based on 181 to 204 months of laboratory monitoring. Except for immersion in leachate and water at 70 and 85ºC, it is far from certain that nominal failure had been reached and even in those cases a conservative interpretation was made. It is expected that

if there had been sufficient material for monitoring longer than 17 years the estimate values would be likely be greater than that reported in this study.

5. Summary and conclusions

An investigation into the degradation of an HDPE GMB immersed air, water and leachate was initiated in 1997, 1997 and 1999, respectively. The first results of this investigation were reported after 2.75 years (Sangam and Rowe 2002) while Rowe et al. (2009) provided a detailed investigation and predictions for Stage I after monitoring the depletion of antioxidants for 8 to 10 years. This paper reports the final results of this 17-year investigation after an additional 7.3 years of ageing at 55, 70 and 85ºC since Rowe et al (2009). The degradation in the SCR, MI and tensile break properties were monitored to assess the degradation Stages II and III and by extension the time to nominal failure. For the GMB and conditions examined in this study, it is concluded that:

1. The MI was not a good indicator for the degradation in the GMB's mechanical properties because: (a) the MI reached negligible values in air after 105 months of ageing whereas, apart from morphological changes, the SCR and tensile break properties did not significantly degrade even after 177 months of ageing (b) MI reached 50% (nominal failure) of the initial value in water and leachate much earlier than either SCR and tensile break properties reached nominal failure. Thus, using MI to interpret Stages II and III would have been very conservative (and was not used).
2. The SCR fluctuated significantly until either reaching nominal failure or the end of the monitoring period. These fluctuations were attributed non-uniform disentanglement of the physical chain entanglements in the amorphous zone of the GMB. The fluctuation in water and leachate were less than that in air.
3. In water, the predicted times to nominal failure varied from > 18 years at 60ºC to >230 years at 35ºC and >1500 years at 20ºC.

4. In the simulated MSW leachate, the predicted times to nominal failure varied from >13 years at 60ºC, to >130 years at 35ºC and >660 years at 20ºC.
5. It was not possible to develop Arrhenius plots for the degradation Stage II and Stage III in air because the degradation in air was very slow such that the nominal failure was not reached based on SCR or the tensile break properties even after ageing the GMB for more than 177 months at temperatures below 85ºC. To provide predictions based on the available data in air, a conservative approach was followed to estimate the degradation stages at 85ºC from the degradation in SCR and tensile break properties using the activation energies for leachate to provide predictions for the times of nominal failure in air. This approach gave times to nominal failure from 170 years at 60ºC to more than 1700 years at 35ºC and lower.
6. Assuming negligible tensile strains in the GMB, the time to nominal failure of this GMB in a composite liner was calculated to vary from >50 years at 60ºC to >550 years at 35ºC and >1100 years at 20ºC.

Although the investigation period at 55ºC was about 17 years, the nominal failure at 55ºC was not reached during the monitoring period and the degradation rates at 55ºC used in the Arrhenius plots for Stage II and Stage III in water and leachate were conservatively estimated. Thus, it is likely that with the monitoring time, the degradation rates at 55ºC used for Stage II and Stage III would decrease and hence the predicted times to nominal failure would increase. Thus, given the conservativeness of the interpretations adopted, these times to nominal failure given above should be regarded as lower bounds; the actual times could be substantially larger. Sadly, even with 17 years of monitoring, this is the best that can be done to define the times to nominal failure for this remarkably good GMB manufactured in 1997.

Acknowledgments

The research presented in this paper was funded by the Natural Science and Engineering Research Council of Canada (NSERC) and used equipment provided by funding from the Canada Foundation for Innovation (CFI) and Ontario Ministry of Research and Innovation. The support of the Killam Trust in the form of a Killam Fellowship to Dr. Rowe is greatly appreciated. The authors are grateful to their industrial partners, Solmax International Inc., Terrafix Geosynthetics Inc., Terrafix Environmental Technologies Inc., TAG Environmental Inc., Ontario Ministry of Environment, the Canadian Nuclear Safety Commission, AECOM, AMEC Earth and Environmental, Golder Associates Ltd., Knight-Piesold, and the CTT group for their participation in, and contributions to, the overarching project. The authors are especially grateful to C. Mitchell and R. Awad for their assistance. Special thanks to Terrafix Geosynthetics and GSE Environmental for providing the GMB used in this study. The authors appreciate the thoughtful review and comments by two anonymous reviewers and B. Ramsay all of which helped improve the paper. The views expressed herein are those of the authors and not necessarily those of the people who have assisted with the research or review of the manuscript.

6. References

Abdelaal, F. B., Rowe, R. K., and Brachman, R. W. I. (2014a). Brittle rupture of an aged HDPE geomembrane at local gravel indentations under simulated field conditions. *Geosynthetic International*, 21(1), 1–23.

Abdelaal, F.B., Rowe, R.K. and Islam, M.Z. (2014b) “Effect of leachate composition on the long-term performance of a HDPE geomembrane”, Geotextiles and Geomembranes, 42(4):348-362. http://dx.doi.org/10.1016/j.geotexmem.2014.06.001

Arab, M.G. (2011) “The integrity of geosynthetic elements of waste containment barrier systems subject to seismic loading”. Ph.D. thesis. School of Sustainable Engineering and the Built Environment, Arizona State University, Tempe, Arizona, USA (2011).

ASTM D1238. Standard Test Method for Flow Rates of Thermoplastics by Extrusion Plastometer. *Annual Book of ASTM Standards*, Philadelphia, USA.

ASTM D1505. Standard Test Method for Density of Plastics by the Density-Gradient Technique, *Annual Book of ASTM Standards*, Philadelphia, USA.

ASTM D3895. Standard Test Method for Oxidative-induction Time of Polyolefins by Differential Scanning Calorimetry. *Annual Book of ASTM Standards*, Philadelphia, USA.

ASTM D5199. Standard Test Method for Measuring the Nominal Thickness of Geosynthetics. *Annual Book of ASTM Standards*, Philadelphia, USA.

ASTM D5261. Standard Test Method for Measuring Mass per Unit Area of Geotextiles. *Annual Book of ASTM Standards,* Philadelphia, USA.

ASTM D5397. Standard Test Method for Evaluation of Stress Crack Resistance of Polyolefin Geomembranes Using Notched Constant Tensile Load Test. *Annual Book of ASTM Standards, Philadelphia*, USA.

ASTM D5885. Standard Test Method for Oxidative Induction Time of Polyolefin Geosynthetics by High-Pressure Differential Scanning Calorimetry. *Annual Book of ASTM Standards, Philadelphia*, USA.

ASTM D6693. Standard Test Method for Determining Tensile Properties of Nonreinforced Polyethylene and Nonreinforced Flexible Polypropylene Geomembranes. *Annual Book of ASTM Standards*, Philadelphia, USA.

ASTM D883. Standard Terminology Relating to Plastics. *Annual Book of ASTM Standards, Philadelphia*, USA.

Benson, C.H. (2017) Characteristics of Gas and Leachate at an Elevated Temperature Landfill, Geotechnical Frontiers 2017 GSP 276, 313-322.

Bolland, J.L. and Gee, G. (1946). Kinetic studies in the chemistry of rubber and related materials. II. The kinetics of oxidation of unconjugated olefins. *Transactions of the Faraday Society*, 42, pp. 236-243.

Brachman, R.W.I., Gudina, S. (2008a) Gravel contacts and geomembrane strains for a GM/CCL composite liner. Geotextiles and Geomembranes, 26(6), 448-459.

Brachman, R.W.I., Gudina, S. (2008b) Geomembrane strains and wrinkle deformations in a GM/GCL composite liner. Geotextiles and Geomembranes, 26(6), 488-497.

Brachman, R.W.I. Sabir, A. (2010) Geomembrane puncture and strains from stones in an underly-ing clay layer. Geotextiles and Geomembranes, 28(4), 335–343.

Brachman, R.W.I. Sabir, A. (2013) Long-term assessment of a layered-geotextile protection layer for geomembranes. Journal of Geotechnical and Geoenvironmental Engineering, 139(5), 752–764.

Dickinson, S., Brachman, R.W.I. (2008) Assessment of alternative protection layers for a GM/GCL composite liner. Canadian Geotechnical Journal, 45(11), 1594-1610.

Eldesouky, H.M.G. and Brachman, R.W.I. (2018) Calculating local geomembrane strains from a single gravel particle with thin plate theory, Geotextiles and Geomembranes, 46(1): 101-110

Ewais, A. M. R. (2014). Longevity of HDPE Geomembranes in Geoenvironmental Applications. (PhD Thesis) Dept. of Civil Engineering, Queen's University, Kingston, Ontario, Canada.

Ewais, A.M.R and Rowe, R.K. (2014a). Effect of ageing on the stress crack resistance of an HDPE geomembrane. *Journal of Polymer Degradation and Stability*, 109, pp. 194-208.

Ewais, A. M. R. and Rowe, R. K. (2014b). Degradation of 2.4 mm-HDPE geomembrane with high residual HP-OIT. 10th International Conference on Geosynthetics – 10ICG, Berlin, Germany, 21 – 25 September 2014.

Ewais, A.M.R. and Rowe, R.K. (2014c). Effect of blown film process on initial properties of HDPE geomembranes of different thicknesses. *Geosynthetics International*, 21(1), pp. 62-82.

Ewais, A.M.R., Rowe, R.K. and Scheirs J. (2014a). Degradation behavior of HDPE geomembranes with high and low initial high pressure oxidative induction time. *Geotextiles and Geomembranes*, 42 (2), pp. 111-126.

Ewais, A.M.R, Rowe, R.K., Brachman, R.W.I. and Arnepalli, D.N. (2014b). Service Life of a High-Density Polyethylene Geomembrane under Simulated Landfill Conditions at 85°C. *ASCE Journal of Geotechnical and Geoenvironmental Engineering*, 140 (11), 04014060.

Fowmes, G.J. (2007). Analysis of steep sided landfill lining systems. Ph.D. thesis, Department of Civil and Building Engineering, Loughborough University, Loughborough, UK.

Fowmes, G.J., Dixon, N., and Jones, D.R.V. (2008a). Validation of a numerical modelling technique for multilayered geosynthetic landfill lining systems. Geotextiles and Geomembranes. 26(2), 109-121.

Fowmes, G.J., Dixon, N. and Jones, D.R.V. (2008b). The influence of horizontal welded seams of geomembrane tension in a steep sided landfill lining system., In Proceedings of the 4th European Geosynthetics Congress. International Geosynthetics Society, Jupiter, FL, USA.

Gallagher,E.M., Tonks,D.M., Shevelan, S., Belton,A.R., Blackmore, R.E. (2016). "Investigations of geomembrane integrity within a 25-year old landfill capping, Geotextiles and Geomembranes, 44(5):770-780GRI-GM13 (2011). Standard Specification for Test Methods, Test Properties and Testing Frequency for High Density Polyethylene (HDPE) Smooth and Textured Geomembranes: GRI Test Method Geomembrane 13, Revision 10: April 11, 2011, *Geosynthetic Research Institute*, Folsom, Pa.

Gassner,F (2017) Development and management of geomembrane liner hippos, Geotextiles and Geomembranes, 45(6):702-706

Giroud, J.P., Tisseau, B., Soderman, K.L., Beech, J.F. (1995) Analysis of strain concentration next to geomembrane seams. Geosynthetics International, 2(6), 1049–1097.

GRI-GM13 (2014). Standard Specification for Test Methods, Test Properties and Testing Frequency for High Density Polyethylene (HDPE) Smooth and Textured Geomembranes: GRI Test Method Geomembrane 13, Revision 10: April 11, 2011, *Geosynthetic Research Institute*, Folsom, Pa.

Gudina, S., Brachman, R.W.I. (2006) Physical response of geomembrane wrinkles overlying compacted clay. Journal of Geotechnical and Geoenvironmental Engineering, 132(10), 1346-1353.

Gugumus, F. (2002). Re-examination of the thermal oxidation reactions of polymers: 2. Thermal oxidation of polyethylene. Polymer Degradation and Stability, 76 (2), pp. 329–340.

Hawkins W.L. (1964). Thermal and oxidative degradation of polymers, Polymer Engineering Science, 4(3), pp. 187–192.

Holström, A. and Sörvik, E.M. (1974). Thermal degradation of polyethylene in a nitrogen atmosphere of low oxygen content. III. Structural changes occurring in low-density polyethylene at oxygen contents below 1.2%. *Journal of Applied Polymer Science*, 18(10), pp. 3153-3178

Hornsey W.P. and Wishaw D.M. (2012). Development of a methodology for the evaluation of geomembrane strain and relative performance of cushion geotextiles. Geotextiles and Geomembranes, 35: 87–99.

Hrapovic, L (2001). Laboratory study of intrinsic degradation of organic pollutants in compacted clayey soil. *Ph.D. dissertation*, Department of Civil and Environmental Engineering, The University of Western Ontario, London, Ontario.

Hsuan, Y.G. (2013). Innovation in Polyolefin Resins Used in Geosynthetics Over the Past 25 Years. *25th edition of the Geosynthetic Research Institute (GSI) conference*, GRI-25.

Hsuan, Y.G. and Koerner, R.M. (1998). Antioxidant depletion lifetime in high density polyethylene geomembranes. *ASCE Journal of Geotechnical and Geoenvironmental Engineering*, 124(6), pp. 532-541.

Hsuan, Y.G., Koerner, R.M., and Lord Jr., A.E. (1993a). Stress cracking resistance of high density polyethylene geomembranes. *Journal of Geotechnical Engineering, ASCE*, 119(11), pp. 1840-1855.

Hsuan, Y.G., Koerner, R.M., and Lord Jr., A.E. (1993b). Notched Constant Tensile Load (NCTL) Test for High-Density Polyethylene Geomembranes. *Geotechnical Testing Journal, ASCE*, 16(4), pp. 1945-7545.

Huang, Y. L. and Brown, N. (1991). Dependence of slow crack growth in polyethylene on butyl branch density: morphology and theory. *Journal of Polymer Science Part B: Polymer Physics*, 29(1), pp. 129-137.

Jones, D.R.V. and Dixon, N. (2005). Landfill lining stability and integrity: the role of waste settlement. Geotextiles and Geomembranes. 23(1), 27-53.

Kavazanjian, E. and Gutierrez, A. (2017). Large scale centrifuge test of a geomembrane-lined landfill subject to waste settlement and seismic loading. Waste Management, 68: 252-262.

Kavazanjian, E., Andresen, J. and Gutierrez, A. (2017). Experimental evaluation of HDPE geomembrane seam strain concentrations. Geosynthetics International. http://dx.doi.org/10.1680/jgein.17.00005

Kavazanjian, E., Wu, X., Arab, M., Matasovic, N. (2018) Development of a numerical model for performance-based design of geosynthetic liner systems. Geotextiles and Geomembranes, In Press.

Koerner, G. (2016). Geosynthetic Institute's Laboratory Accreditation Program: a Twenty year Review. Proceedings of GeoAmericas, Miami, Florida, USA.

Koerner, R.M., Lord, A.E., and Hsuan, Y.H. (1992). Arrhenius modeling to predict geosynthetic degradation. *Geotextiles and Geomembranes*, 11(2), pp. 151-183.

Kuroki, T., Sawaguchi, T., Niikuni, S. and Ikemura, T. (1982). Mechanism for long-chain branching in the thermal degradation of linear high-density polyethylene. Macromolecules, 15(6), pp. 1460-1464.

MoE (1998). Landfill standards: a guideline on the regulatory and approval requirements for the new or expanding landfilling sites, Ontario Ministry of the Environment, Ontario Regulation 232/98, Queen's Printer for Ontario, Toronto.

Müller, W. and Jacob, I. (2003). Oxidative resistance of high density polyethylene geomembranes. *Polymer Degradation and Stability*, 79(1), pp. 161-172.

Müller, W.W., 2007. HDPE Geomembranes in Geotechnics. Springer Verlag, Heidelberg, Germany. 486pp.

Myers, D., 1988. Surfactant Science and Technology. VCH Publishers, New York. 351pp.

Osawa, Z., 1992. Photo-induced degradation of polymers. In: Hamid, A.H., Amin, M.B., Maadah, A.G. (Eds.), *Handbook of Polymer Degradation*. Marcel Dekker Inc., New York, pp. 169–217.

Peacock, A. (2000). Handbook of Polyethylene: Structures, Properties and Application, *Marcel Dekker Inc*, New York, 534p.

Ramsey, B., Zimmel, E. and Zanzinger, H. (2018) "New technique for predictive geomembrane stress crack performance: commercial application", 11th International Conference on Geosynthetics, Seoul, Korea, November.

Reinhart, D.R., Mackey, R. Levin, S., Joslyn, R. and Motlagh, A. (2017) Field Investigation of an Elevated Temperature Florida Landfill, Geotechnical Frontiers 2017 GSP 276, 298-301

Rowe R.K. 2005. Long-term performance of contaminant barrier systems. Géotechnique, 55(9): 631-678.

Rowe, R.K. (2012). Short and long-term leakage through composite liners. The 7th Arthur Casagrande Lecture. *Canadian Geotechechnical Journal,* 49(2), pp. 141-169.

Rowe, R.K. and Ewais, A.M.R. (2014). Antioxidant depletion from five geomembranes of same resin but of different thicknesses immersed in leachate. Geotextiles and Geomembranes, 42 (5), pp. 540–554.

Rowe, R.K. and Ewais, A.M.R. (2015). Ageing of exposed HDPE geomembranes at locations with different climatological conditions. Canadian Geotechnical Journal, 52 (3), pp. 326-343

Rowe, R.K. Sangam, H.P. and Lake, C.B (2003). "Evaluation of an HDPE geomembrane after 14 years as a leachate lagoon liner", Canadian Geotechnical Journal, 40(3):536-550.

Rowe, R.K., Quigley, R.M., Brachman, R. W. I. and Booker, J.R. (2004). Barrier Systems for Waste Disposal Facilities, *E & FN Spon*, London, 587p.

Rowe, R.K., Islam, M.Z. and Hsuan, Y.G. (2008). "Leachate chemical composition effects on OIT depletion in HDPE geomembranes", *Geosynthetics International*, **15**(2):136-151

Rowe, R.K. and Rimal, S. (2008) "Depletion of antioxidant from HDPE geomembrane in a composite liner", ASCE Journal of Geotechnical and Geoenvironmental Engineering **134**(1):68-78.

Rowe, R.K., Rimal, S. and Sangam, H.P. (2009). Ageing of HDPE geomembrane exposed to air, water and leachate at different temperatures. *Geotextiles and Geomembranes*, 27(2), pp. 131-151.

Rowe, R.K., Islam, M.Z., Brachman, R.W.I., Arnepalli, D.N. and Ewais, A.M.R. (2010). Antioxidant depletion from an HDPE geomembrane under simulated landfill conditions. *ASCE Journal of Geotechnical and Geoenvironmental Engineering*, 136(7): 930-939.

Rowe, R.K., Chappel, M.J., Brachman, R.W.I. and Take, W.A. (2012). "Field monitoring of geomembrane wrinkles at a composite liner test site", Canadian Geotechnical Journal, 49(10): 1196-1211.

Rowe, R.K., Abdelaal, F.B. and Brachman, R.W.I. 2013. Antioxidant depletion from an HDPE geomembrane with a sand protection layer. Geosynthetics International, 20(2): 73-89.

Rowe, R.K., Abdelaal, F.B. and Islam, M.Z. (2014) "Aging of HDPE geomembrane of three different thicknesses", ASCE J*ournal of Geotechnical and Geoenvironmental Engineering*, 140(5): 4014005-1 to 4014005-11, DOI: 10.1061/(ASCE)GT.1943-5606.0001090

Sabir, A. and Brachman, R.W.I. (2012). Time and temperature effects on geomembrane strain from a gravel particle subject to sustained vertical force. Canadian Geotechnical Journal, 49(3): 249-263.

Sangam, H. P. and Rowe, R. K. (2002). Effects of exposure conditions on the depletion of antioxidants from high-density polyethylene (HDPE) geomembranes. *Canadian Geotechnical Journal*, 39(6), pp. 1221-1230.

Scheirs, J. (2000). Compositional and Failure Analysis of Polymers: A Practical Approach, John Wiley & Sons, Ltd, Chichester, UK, pp. 766.

Scheirs, J. (2009). A guide to polymeric geomembranes: A practical approach. *John Wiley and Sons*, Ltd, Australia, 572 p.

Seeger, S. and Müller, W. (2003). Theoretical approach to designing protection: selecting a geomembrane strain criterion. Geosynthetics: Protecting the Environment, Dixon, N., Smith, D. M., Greenwood, J. H. & Jones, D. R. V., Editors, Thomas Telford, London, UK:137-152.

Shenoy, A.V. and Saini, D.R. (1986). Melt flow index: more than just a quality control rheological parameter. part I. *Advances in Polymer Technology*, 6(1), pp.1-58.

Sia, A.H.I. and Dixon, N. (2012). Numerical modelling of landfill lining system waste interaction: implications of parameter variability. Geosynthetics International. 19(5): 393-408.

Stark, T.D., Martin, J.W., Gerbasi, G.T., Thalhamer, T., and Gortner, R.E. (2012). Aluminum waste reaction indicators in a Municipal Solid Waste Landfill. *ASCE Journal of Geotechnical and Geoenvironmental Engineering*, 138(3): 252-261.

Stark, T.D. and Jafari, N.H. (2017) Landfill operational techniques in the presence of elevated temperatures, Geotechnical Frontiers 2017 GSP 276, 289-297.

Take, W.A, Watson, E., Brachman, R.W.I., and Rowe, R.K. (2012) "Thermal expansion and contraction of geomembrane liners subjected to solar exposure and backfilling", ASCE Journal of Geotechnical and Geoenvironmental Engineering, 138(11): 1387 – 1397.

Thusyanthan, N.I., Madabhushi, S.P.G., and Singh, S. 2007. Tension in geomembranes on landfill slopes under static and earthquake loading - Centrifuge study. Geotextiles and Geomembranes, 25(2): 78-95.

Viebke, J., Elble, E., Ifwarson, M. and Gedde U.W. (1994). Degradation of unstabilized medium-density polyethylene pipes in hot-water applications. *Polymer Engineering and Science*, 34(17), pp. 1354-1361.

Winslow, F.H., Hellman, M.Y., Matreyek, W. and Stills, S.M. (1966). Autoxidation of semicrystalline polyethylene. *Polymer Engineering and Science*, 6(3), pp. 273-278.

Wu, X. (2013). Effect of waste settlement and seismic loading on the integrity of geosynthetic barrier systems. Masters' thesis, School of Sustainable Engineering and the Built Environment, Arizona State University, Tempe, Arizona, USA.

Yang, P., Xue, S.B., Song, L., and Zhu, X.W. (2017). Numerical simulation of geomembrane wrinkle formation. Geotextiles and Geomembranes, 45(6): 697-701.

Yu, Y. and Rowe, R.K. (2018a) "Modelling deformation and strains induced by waste settlement in a centrifuge test", Canadian Geotechnical Journal, (in press) https://doi.org/10.1139/cgj-2017-0558

Yu, Y. and Rowe, R.K. (2018b) "Development of Geomembrane Strains in Waste Containment Facility Liners with Waste Settlement", Geotextiles and Geomembranes, 46 (2) 226-242. https://doi.org/10.1016/j.geotexmem.2017.11.004

Zamara, K.A., Dixon, N., Fowmes, G., Jones, D.R.V., and Zhang, B. (2014). Landfill side slope lining system performance: A comparison of field measurements and numerical modelling analyses. Geotextiles and Geomembranes, 42(3): 224-235.

NOTATION

High density polyethylene HDPE	HDPE
Geomembrane	GMB
Stress crack resistance	SCR
Initial stress crack resistance	SCR_o
Melt Index	MI
Tensile break elongation	TBE
Tensile break strength	TBS
Municipal solid waste	MSW
Time to nominal failure	t_{NF}
Times to nominal failure of a GMB in leachate, air and water exposures	$t_{f\ (leachate)}$, $t_{f\ (air)}$ and $t_{f\ (water)}$
Length Stage I	Δt_I
Length Stage II	Δt_{II}
Length Stage III	Δt_{III}
Degradation rate of the GMB property of interest during Stage II and Stage III respectively, in months^{-1}	η and γ
Degradation rate in months^{-1}	s
Activation energy (J.mol^{-1}) required by the reactants to react	E_a
Universal gas constant (8.314 J.mol^{-1}.K^{-1})	R
Absolute temperature in Kelvin	T

Table 1. GMB Properties (modified from Rowe et al. 2009).

Property	Method	Units	Value
Nominal thickness	ASTM D5199	mm	2.0
GMB Density	ASTM D1505	g/cm^3	0.94 (0.3)
Std-OIT	ASTM D3895	min	134 (3.7)
HP-OIT	ASTM D5885	min	380 min
MI (2.16 kg/190^{0}C)	ASTM D1238	g/10min	0.42 (1.5)
HLMI (21.6 kg/190^{0}C)	ASTM D1238	g/10min	12.1 (0.8)
HLMI/MI		ratio	28.8
Tensile properties for specimens type IV taken in machine direction (ASTM D6693)			
Strength at yield		kN/m	33.9 (0.9)
Strength at break		kN/m	80.5 (3.2)
Strains at yield		%	22 (1.6)
Strains at break		%	1034(6)
Tensile properties for specimens type IV taken in cross-machine direction (ASTM D6693).			
Strength at yield		kN/m	34 (2.2)
Strength at break		kN/m	79.6 (3.9)
Strains at yield		%	23 (0.7)
Strains at break		%	1012 (6.7)
SCR	ASTM D5397	hours	5220 (3)

Note: numbers in brackets are the coefficient of variation in percent.

Table 2. Estimated degradation Stages in months in all incubations.

Property	Exposure	Temperature / Stages	85 ºC	70 ºC	55 ºC
OIT	**Air**	**Stage I**[1]	27	87	194
	Water		24	38	118
	Leachate		10	17[2]	23
SCR	**Air**	**Stage II**	37	> 70	>> 70
		Stage III	113	nd[3]	nd
		t_{NF}	177	> 177	>> 177
	Water	**Stage II**	9	30	> 143
		Stage III	3	7	108
		t_{NF}	36	75	> 368
	Leachate	**Stage II**	9	30	≥ 143
		Stage III	3	7	108
		t_{NF}	22	54[2]	> 274
Tensile Break Elongation	**Air**	**Stage II**	37	> 70	>> 70
		Stage III	193	nd	nd
		t_{NF}	257	> 257	>> 257
	Water	**Stage II**	12	46	> 86
		Stage III	2	11	nd
		t_{NF}	38	95	nd
	Leachate	**Stage II**	18	30	104
		Stage III	8	13	164
		t_{NF}	36	50[2]	291
Break Tensile Strength	**Air**	**Stage II**	37	> 70	>> 70
		Stage III	201	nd	nd
		t_{NF}	265	> 265	>> 265
	Water	**Stage II**	9	42	> 86
		Stage III	8	15	nd
		t_{NF}	42	95	nd
	Leachate	**Stage II**	18	30	104
		Stage III	11	29	158
		t_{NF}	39	76[2]	285

[1]Stage I calculated based on the rates estimate by Rowe et al. (2009) and a residual OIT value of 2min.
[2] Stage I extrapolated form data in Rowe et al. (2009).
[3]nd =no determined due to absence of data in this stage due to the very slow rate of degradation

Table 3. Predicted degradation stages and times to nominal failure (years) in leachate at different temperatures based on the conservative interpretation of the data. The predicted values were estimated from Arrhenius plots based on different properties listed below (numbers rounded to no more than three significant digits for Stages I, II and III, and to two significant digits for t_{NF} and hence numbers may not add up exactly due to rounding).

Immersed in leachate		Time (years)						
Property	**Temperature (ºC)**	**60**	**50**	**45**	**40**	**35**	**30**	**20**
OIT	**Stage I**[1]	2.6	4.0	5.0	7.0	9.0	12	23
SCR	**Stage II = 1/η**	7.0	19	32	56	98	175	594
	Stage III = 1/γ	3.6	13	26	54	110	238	1170
	Time to nominal failure = Stage I + Stage II + Stage III	13	36	63	120	220	420	1700[2]
	Stages (II + III) = 1/δ	10.9	33	59	108	200	380	1460
	Time to nominal failure = Stage I + Stages (II + III)	13	37	64	120	210	390	1500
Tensile Break Elongation	**Stage II = 1/η**	5.7	11	15	21	31	44	96
	Stage III = 1/γ	5.8	18	32	58	107	202	776
	Time to nominal failure = Stage I + Stage II + Stage III	14	33	52	86	150	260	900
Tensile Break Strength	**Stage II = 1/η**	5.7	11	15	21	31	44	96
	Stage III = 1/γ	7.4	20	33	55	95	166	540
	Time to nominal failure = Stage I + Stage II + Stage III	16	35	53	83	130	220	660
Minimum time to nominal failure, t_{NF}		13	33	52	83	130	220	660

[1]From Rowe et al. (2009).

[2] It is not considered advisable to extrapolate more than two orders of magnitude greater than the testing period (i.e., 1700 years) so all larger extrapolated numbers are reported at 1700 years.

Table 4. Predicted degradation stages and time to nominal failure (years) in water at different temperatures. The predicted values were estimated from Arrhenius plots based on different properties listed below (numbers rounded to no more than three significant digits for Stages I, II and III, and to two significant digits for t_{NF} and hence numbers may not add up exactly due to rounding).

Immersed in water		Time (years)						
Property	**Temperature (ºC)**	**60**	**50**	**45**	**40**	**35**	**30**	**20**
OIT	**Stage I**[1]	7.3	13	17	23	31	43	83
SCR	**Stage II = 1/η**	7.0	19	32	56	98	175	594
	Stage III = 1/γ	3.6	13	26	54	112	238	1170
	Time to nominal failure = Stage I + Stage II + Stage III	18	45	75	130	240	460	1700[2]
	Stages (II + III) = 1/δ	10.9	33	59	108	200	380	1460
	Time to nominal failure = Stage I + Stages (II + III)	18	46	76	130	230	420	1500
Tensile Break Elongation	**Stage II = 1/η**	10.1	28	48	83	147	265	914
	Stage III = 1/γ	3.1	11	22	45	93	197	947
	Time to nominal failure = Stage I + Stage II + Stage III	21	52	87	150	270	500	1700[2]
Tensile Break Strength	**Stage II = 1/η**	10.5	34	63	119	228	448	1700[2]
	Stage III = 1/γ	2.0	3	4	5	7	9	16
	Time to nominal failure = Stage I + Stage II + Stage III	20	50	84	150	270	500	1700[2]
Minimum time to nominal failure, t_{NF}		18	45	75	130	230	420	1500

[1]From Rowe et al. (2009).

[2] It is not considered advisable to extrapolate more than two orders of magnitude greater than the testing period (i.e., 1700 years) so all larger extrapolated number are reported at 1700 years.

Table 5. Predicted degradation stages and times to nominal failure (years) in air at different temperatures. The predicted values were evaluated using Equation (7) and Ea/R estimated for the relative property in leachate. (Numbers rounded to no more than three significant digits for Stages I, II and III, and to two significant digits for t_{NF} and hence numbers may not add up exactly due to rounding).

Immersed in air		Time (years)						
Property	**Temperature (°C)**	**60**	**50**	**45**	**40**	**35**	**30**	**20**
OIT	**Stage I**[1]	12	21.7	30	41	57	80	163
SCR	**Stages (II + III) = 1/δ**	153	464	829	1510	1700[2]	1700[2]	1700[2]
	Time to nominal failure = Stage I + Stages (II + III)	170	490	860	1500	1700[2]	1700[2]	1700[2]
Tensile Break Elongation	**Stage II = 1/η**	13	25	35	49	71	102	222
	Stage III = 1/γ	196	595	1060	1700[2]	1700[2]	1700[2]	1700[2]
	Time to nominal failure = Stage I + Stage II + Stage III	220	640	1100	1700[2]	1700[2]	1700[2]	1700[2]
Tensile Break Strength	**Stage II = 1/η**	13	25	35	49	71	102	222
	Stage III = 1/γ	150	398	660	1120	1700[2]	1700[2]	1700[2]
	Time to nominal failure = Stage I + Stage II + Stage III	170	440	730	1200	1700[2]	1700[2]	1700[2]
Minimum time to nominal failure[2], t_{NF}		170	440	730	1200	>1700	>1700	>1700

[1]From Rowe et al. (2009).

[2] It is not considered advisable to extrapolate more than two orders of magnitude greater than the testing period (i.e., 1700 years) so all larger extrapolated number are reported at 1700 years.

Table 6. Comparison of observed (Table 2) and predicted (Tables 4-6) times to nominal failure at the three test temperatures

	Leachate				Water			
	Stage II		Stage III		Stage II		Stage III	
T (ºC)	Observed	Predicted	Observed	Predicted	Observed	Predicted	Observed	Predicted
SCR								
55ºC	12	12	9.0	6.8	12	12	9.0	6.8
70ºC	2.5	2.7	0.6	1.0	2.5	2.7	0.6	1.0
85ºC	0.8	0.7	0.3	0.2	0.8	0.7	0.3	0.2
TBS								
55ºC	8.7	7.8	13	12		19		2.5
70ºC	2.5	3.1	2.4	3.0	3.5	3.5	1.3	1.3
85ºC	1.5	1.3	0.9	0.8	0.8	0.7	0.7	0.7
TBE								
55ºC	8.7	7.8	14	10		17		5.9
70ºC	2.5	3.1	1.1	2.1	3.8	3.8	0.9	0.9
85ºC	1.5	1.3	0.7	0.5	1.0	1.0	0.2	0.2

Table 7. Predicted times to nominal failure for the tested geomembrane aged in composite liner using Equ. 2 and number given in Tables 3-5

	Time nominal failure[1], t_{NF} (years)						
Temperature (ºC) / Property	60	50	45	40	35	30	20
Stress crack resistance	54	150	270	470	590	720	1600
Tensile break elongation	54	150	270	470	590	720	1600
Tensile break strength	56	140	230	380	560	660	1200
Very conservative minimum[2]	54	140	230	370	550	640	1100

[1] Predictions are based on the summation of Stage I and II +III.

[2] The calculated form Equ.2 based on the minimum t_{NF} given in Tables 3-

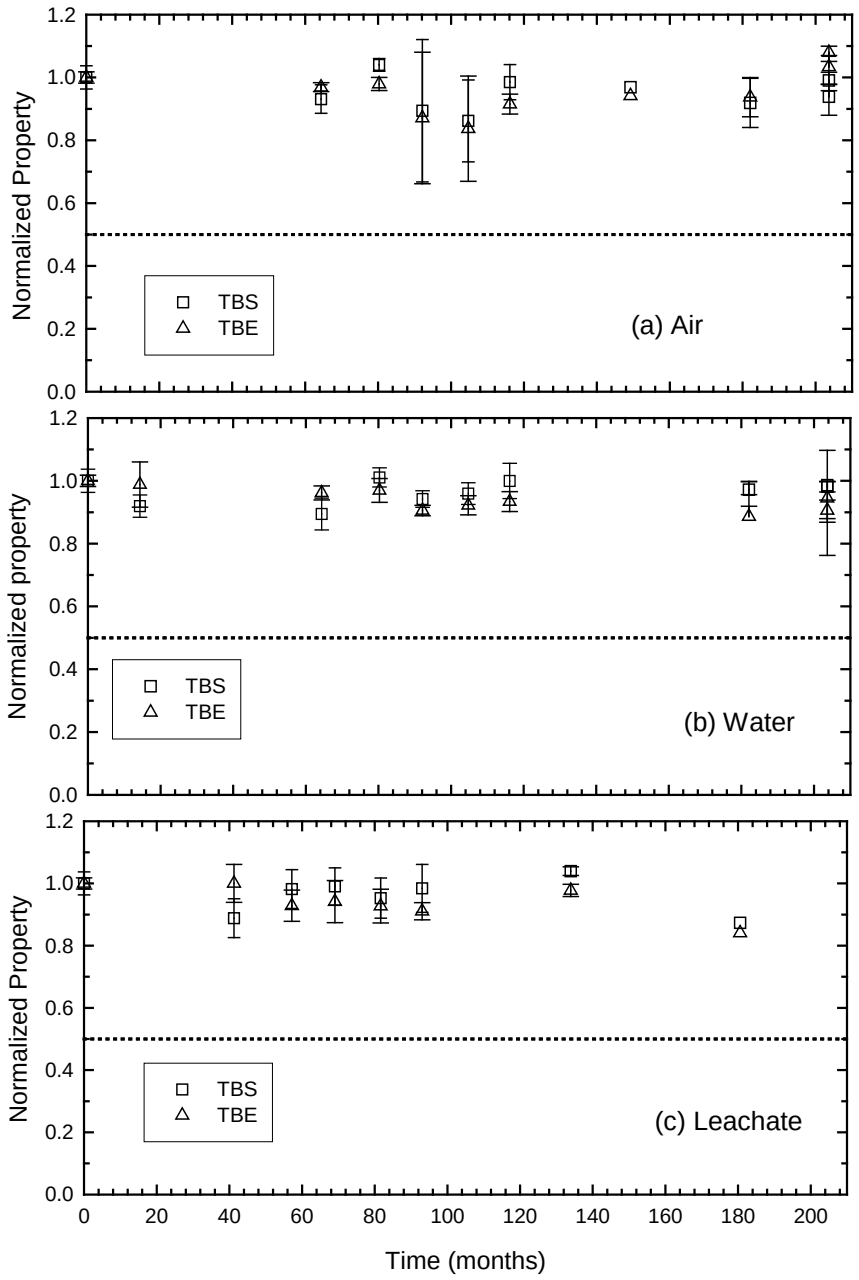

Figure 1. Changes in tensile break strength and elongation with time for GMB samples aged in air, water and leachate at 55ºC. Error bars of the data reported after 116, 116 and 110 months in air, water and leachate, respectively, represent the maximum and minimum values measured for the reported property. The data before these times were reported in Rowe et al. (2009).

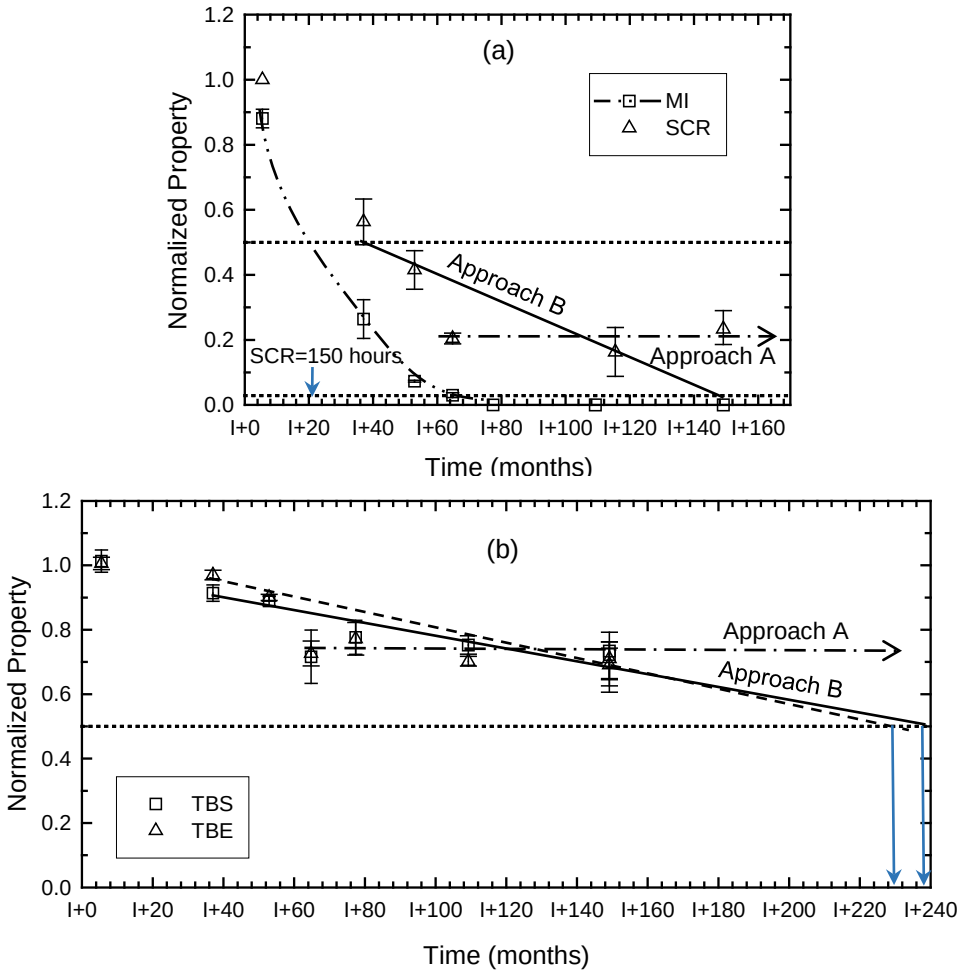

Figure 2. Aged in air at 85°C: Change in: (a) SCR and MI and (b) TBS and TBE, with time. "I" refers to Δt_I. The sloping solid and dashed lines are conservative interpretation for the degradation of the mechanical properties following Approach B. The horizontal dash-dotted line is less conservative interpretation following Approach A (as may indeed be the case) that the decrease was due to morphological change and the properties are still in Stage II. Error bars after I+90 months represent the maximum and minimum values measured for the reported property. The data before I+90 months were reported in Rowe et al. (2009).

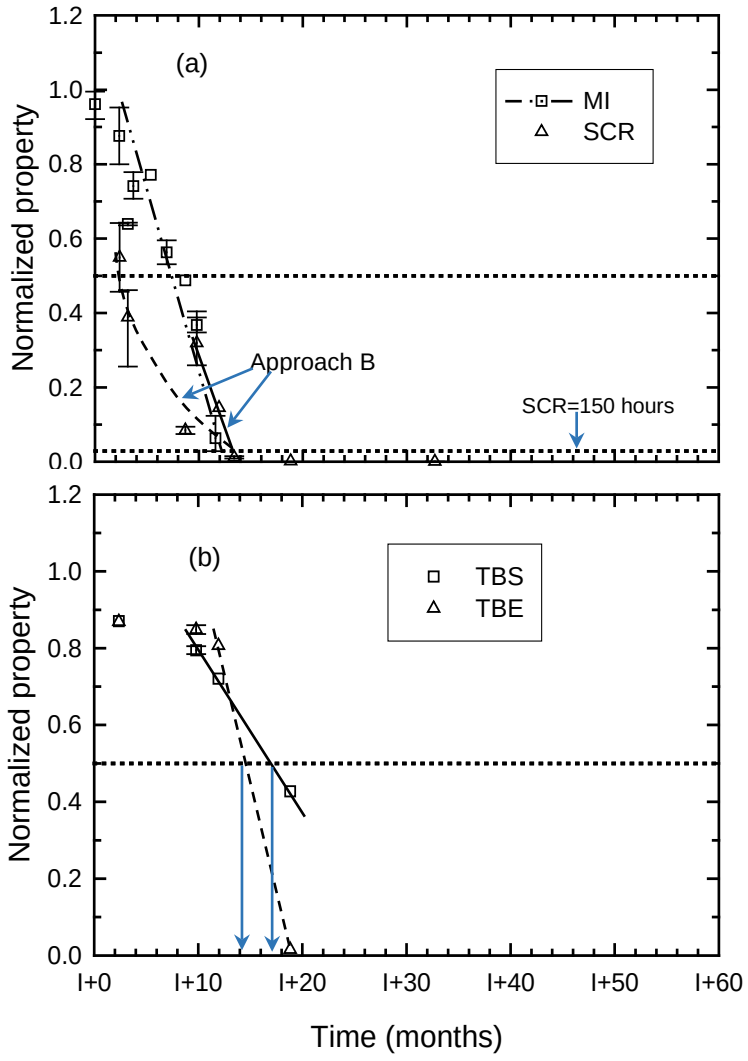

Figure 3. Aged in water at 85°C: (a) SCR with different (dashed and solid) fittings following Approach B and MI, and (b) TBS and TBE fitted with solid and dashed lines, respectively following Approach B. "I" refers to Δt_I. Error bars represent the maximum and minimum values measured for the reported property.

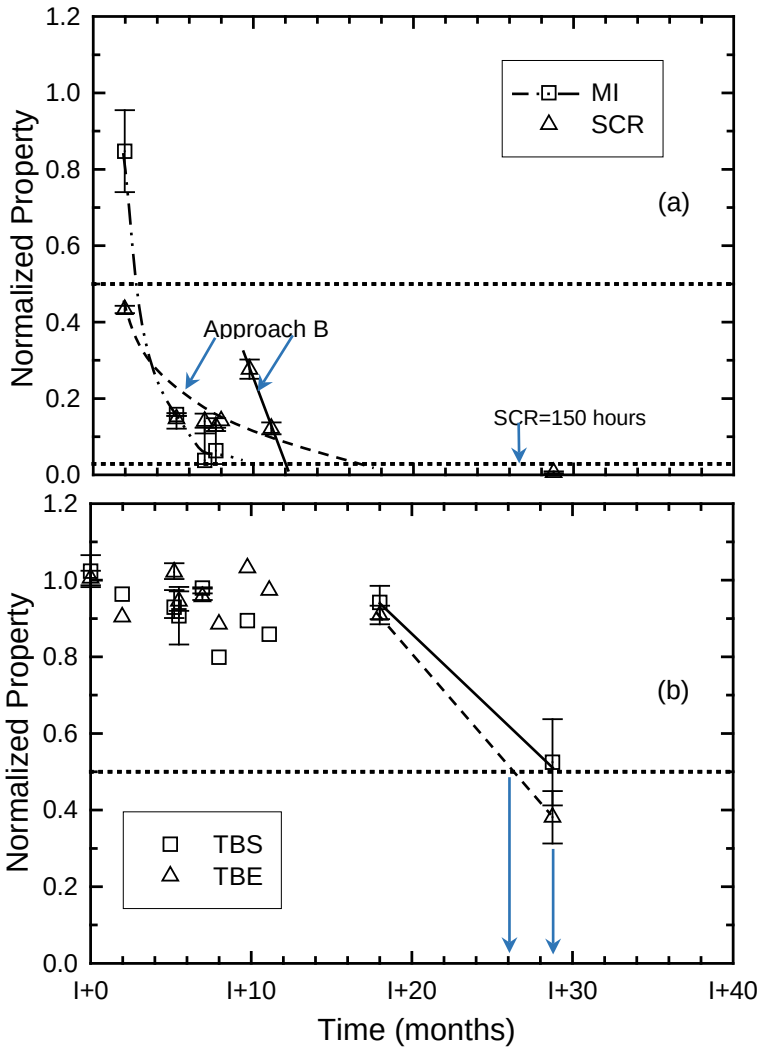

Figure 4. Aged in leachate at 85°C: (a) SCR with different (dashed and solid) fittings following Approach B and MI, and (b) TBS and TBE fitted with solid and dashed lines, respectively following Approach B. "I" refers to Δt_I. Error bars represent the maximum and minimum values measured for the reported property.

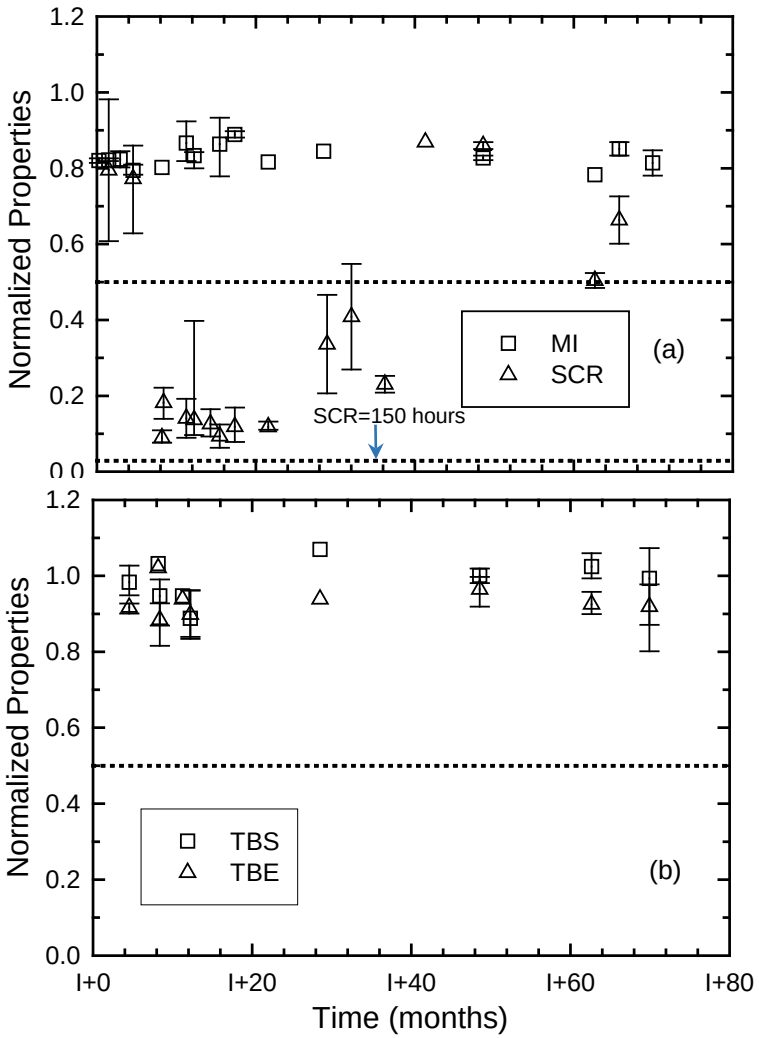

Figure 5. Aged in air at 70ºC: (a) SCR and MI, and (b) TBS and TBE. "I" refers to Δt_I. Error bars represent the maximum and minimum values measured for the reported property.

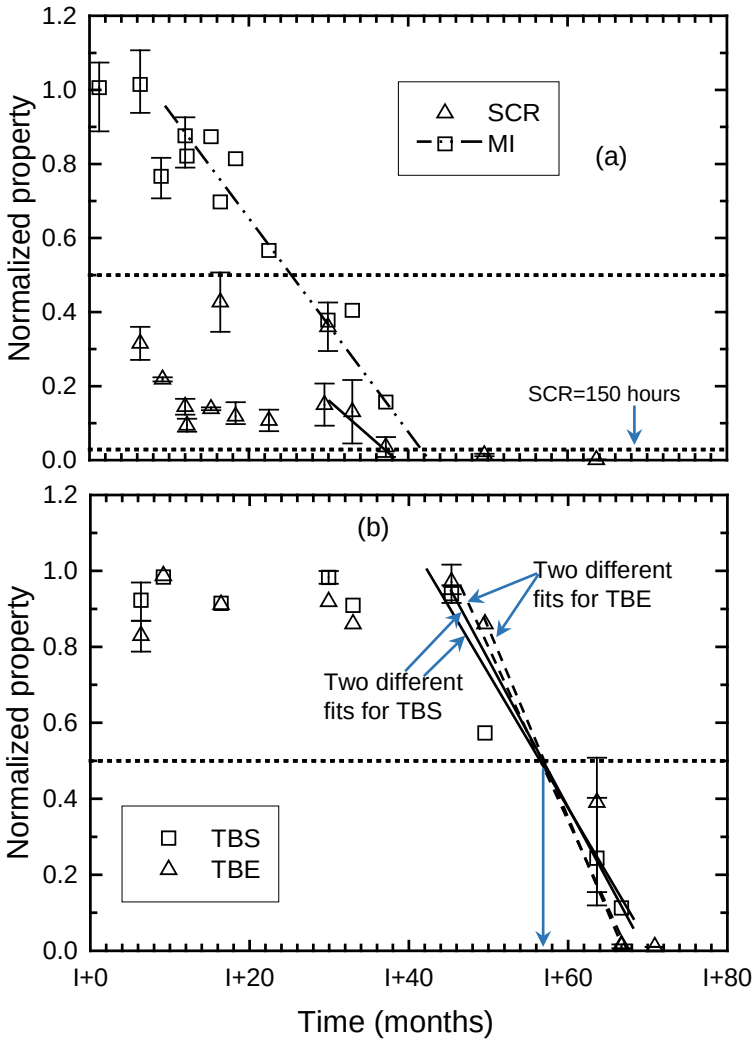

Figure 6. Aged in water at 70°C: (a) SCR and MI, and (b) TBS and TBE fitted with solid and dashed lines, respectively following Approach B. Two different fits for each tensile property were made. "I" refers to Δt_I. Error bars represent the maximum and minimum values measured for the reported property.

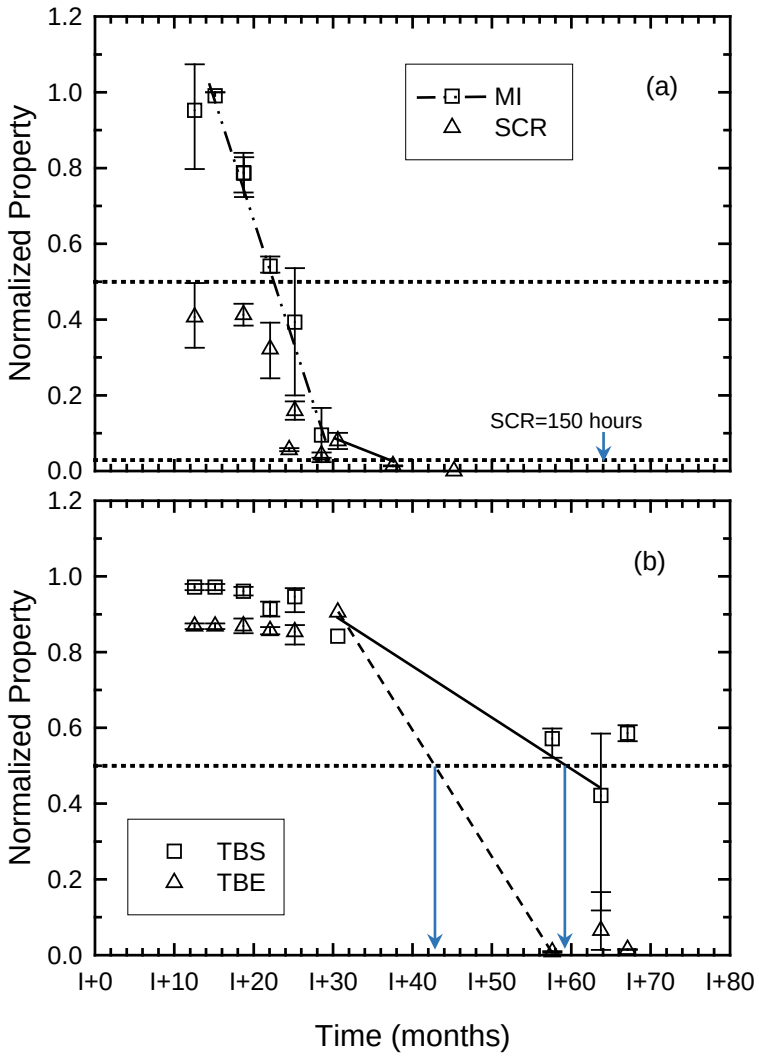

Figure 7. Aged in leachate at 70°C: (a) SCR and MI, and (b) TBS and TBE fitted with solid and dashed lines, respectively following Approach B. "I" refers to Δt_I. Error bars represent the maximum and minimum values measured for the reported property.

.

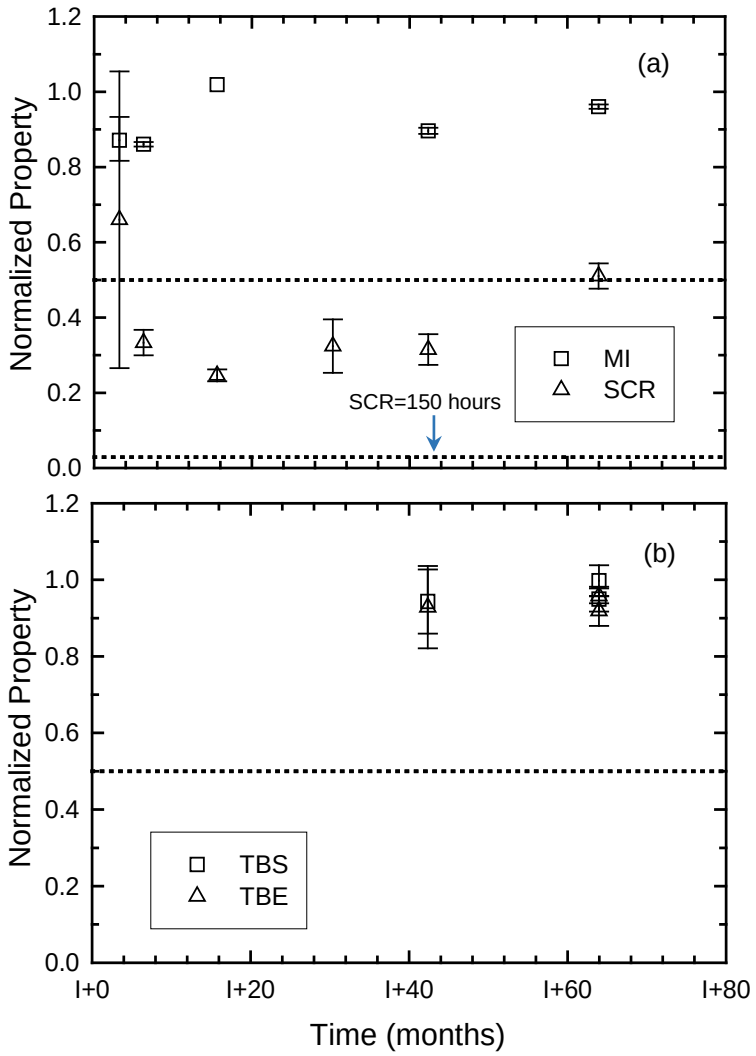

Figure 8. Aged in air at 55°C: (a) SCR and MI, and (b) TBS and TBE. "I" refers to Δt_I. Error bars represent the maximum and minimum values measured for the reported property.

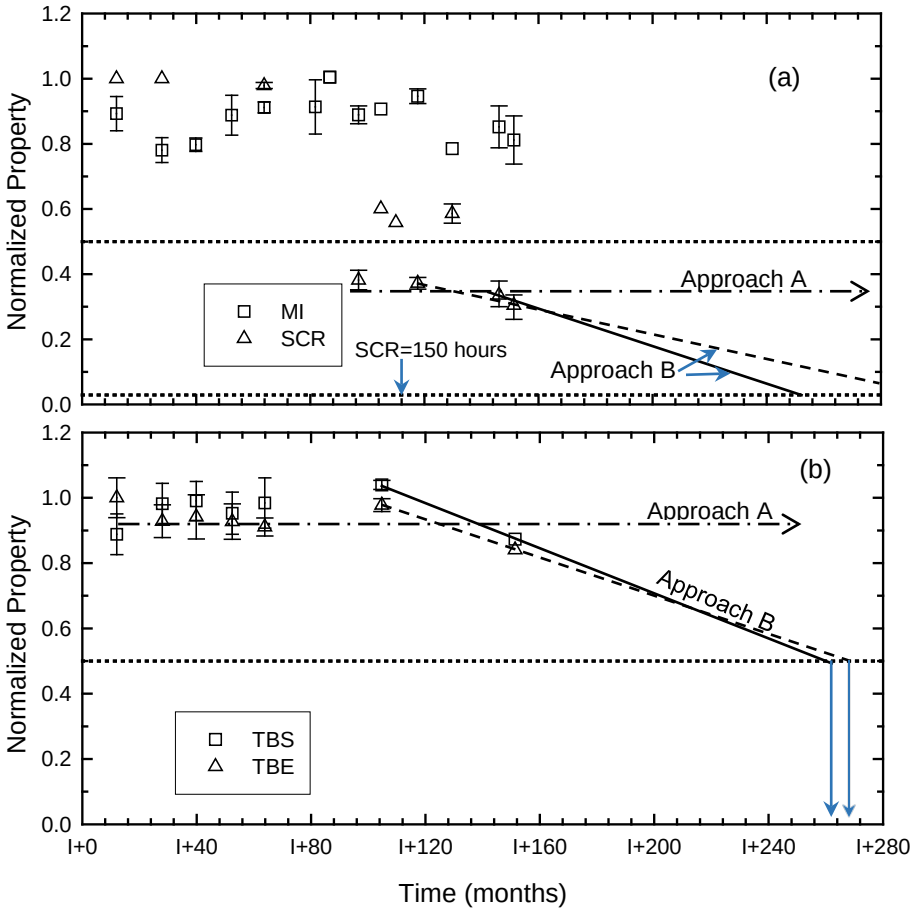

Figure 9. Aged in leachate at 55ºC: (a) SCR and MI, and (b) tensile break strength and elongation "I" refers to the length of Stage I. The sloping solid and dashed lines are conservative interpretation for the degradation of the mechanical properties following Approach B. The horizontal dash-dotted line is less conservative interpretation following Approach A (as may indeed be the case) that the decrease was due to morphological change and the properties are still in Stage II. Error bars after I+87 months represent the maximum and minimum values measured for the reported property.

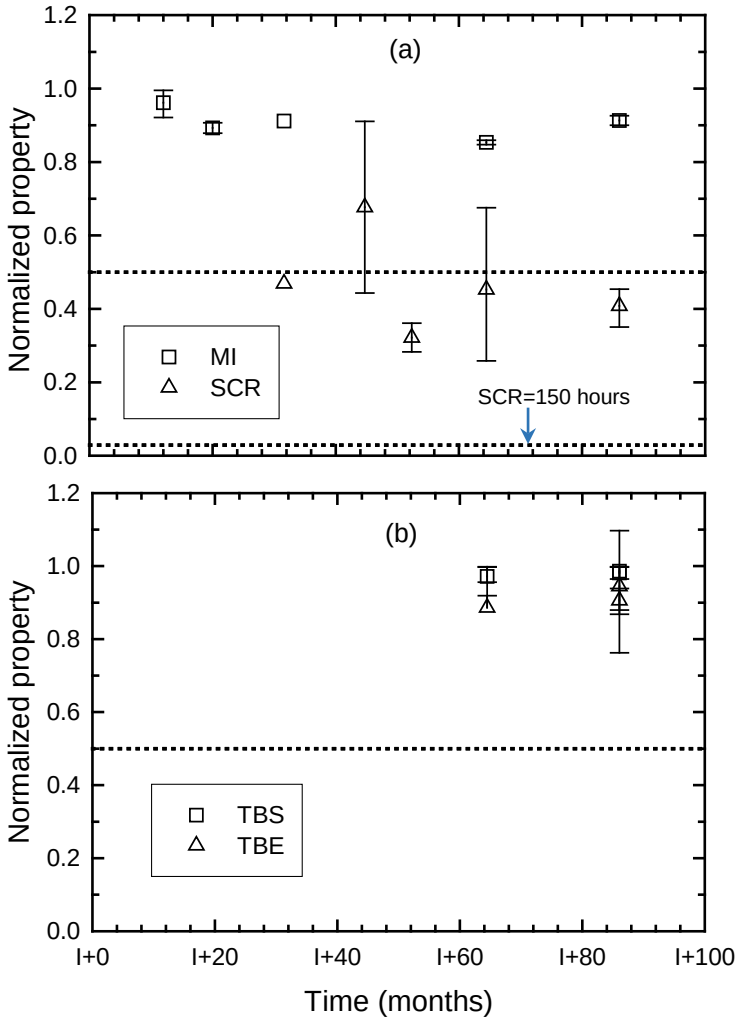

Figure 10. Aged in water at 55°C: (a) SCR and MI, and (b) TBS and TBE. "I" refers to Δt_I. Error bars represent the maximum and minimum values measured for the reported property.

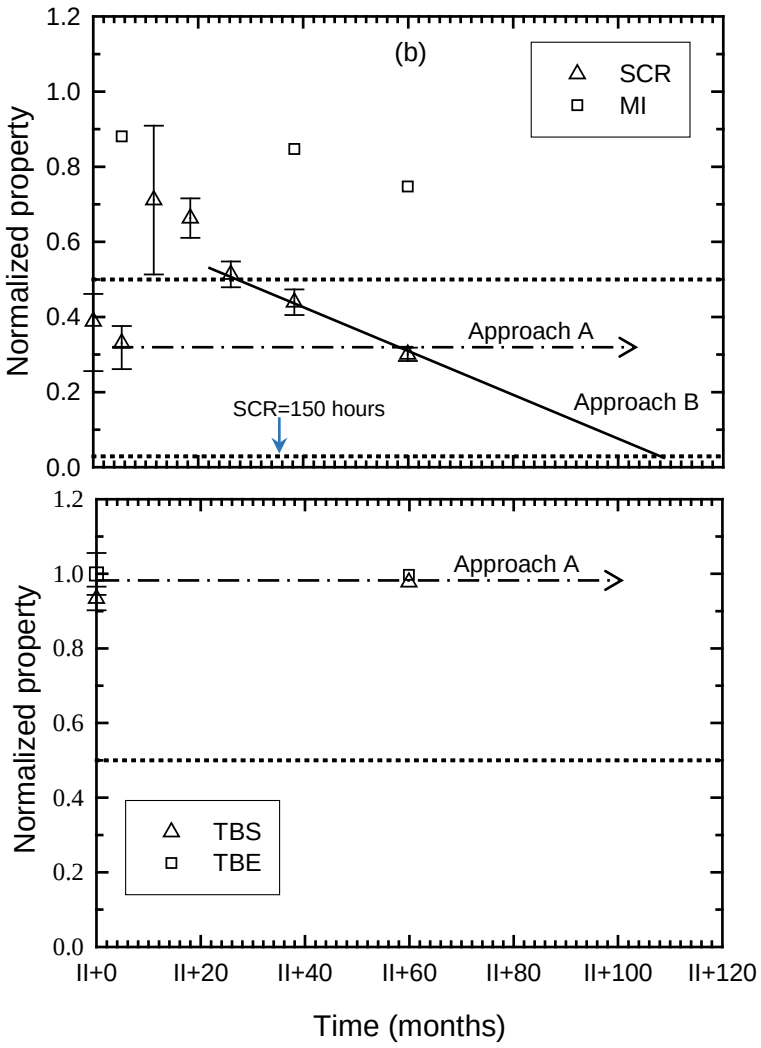

Figure 11. Aged in water at 55ºC: (a) SCR and MI, and (b) TBS and TBE. "II" refers to Δt_{II}.. The sloping solid line are conservative interpretation for the degradation in SCR following Approach B. The horizontal dash-dotted line is less conservative interpretation following Approach A (as may indeed be the case) that the decrease was due to morphological change and the properties are still in Stage II. Error bars represent the maximum and minimum values measured for the reported property.

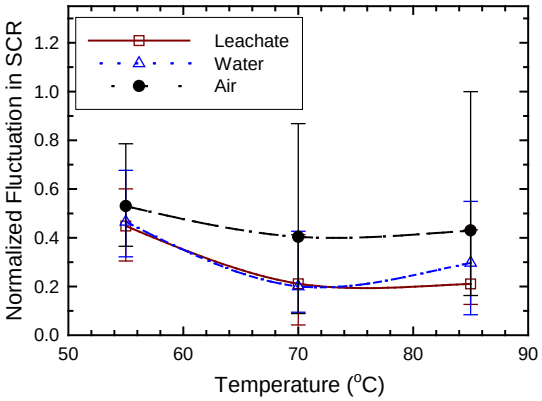

Figure 12. Fluctuation in SCR during the monitoring period with respect to temperature in air, water and leachate.

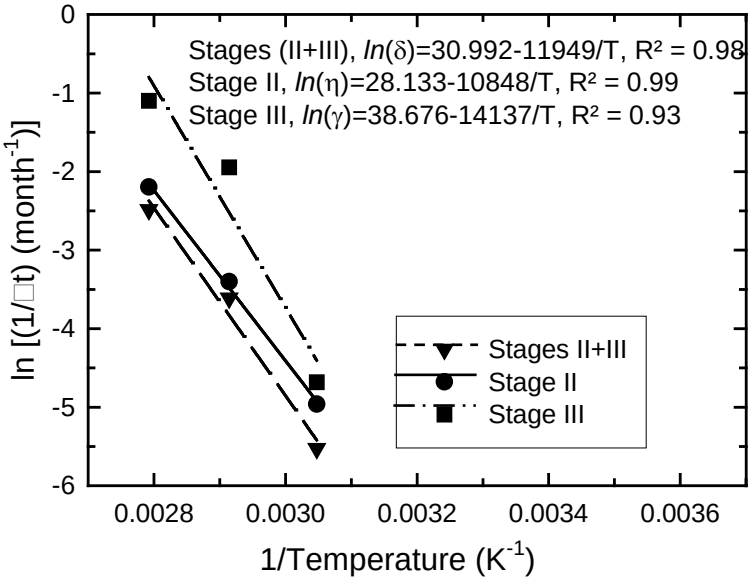

Figure 13. Arrhenius plot for Stage II, Stage III and Stages II+III in leachate and water based on SCR.

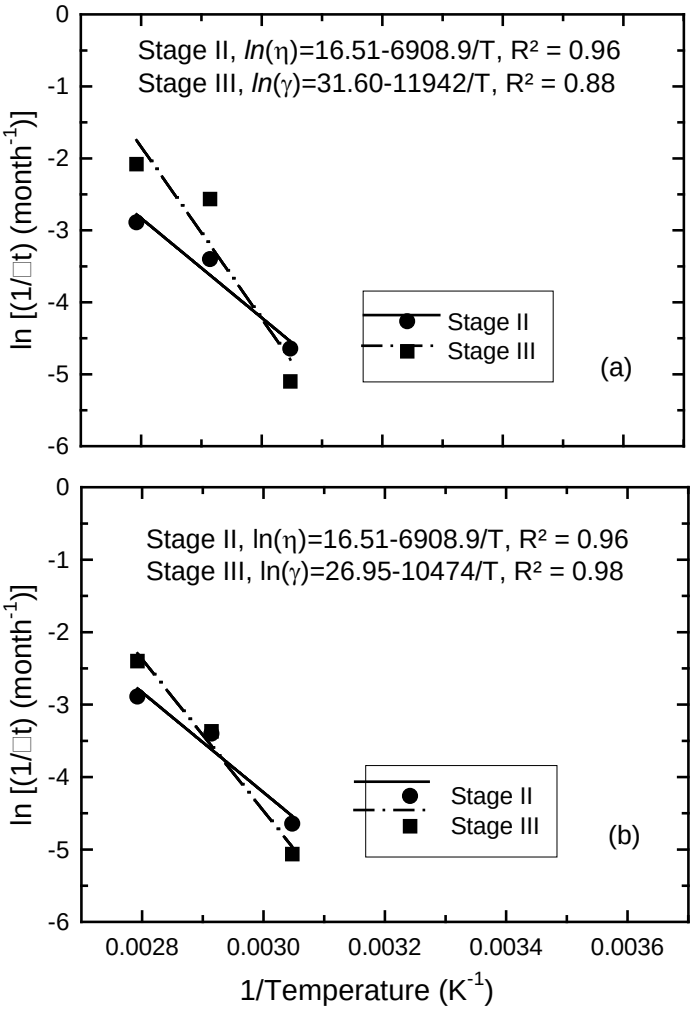

Figure 14. Arrhenius plot for Stage II and Stage III in leachate based on tensile break: (a) elongation and (b) strength.

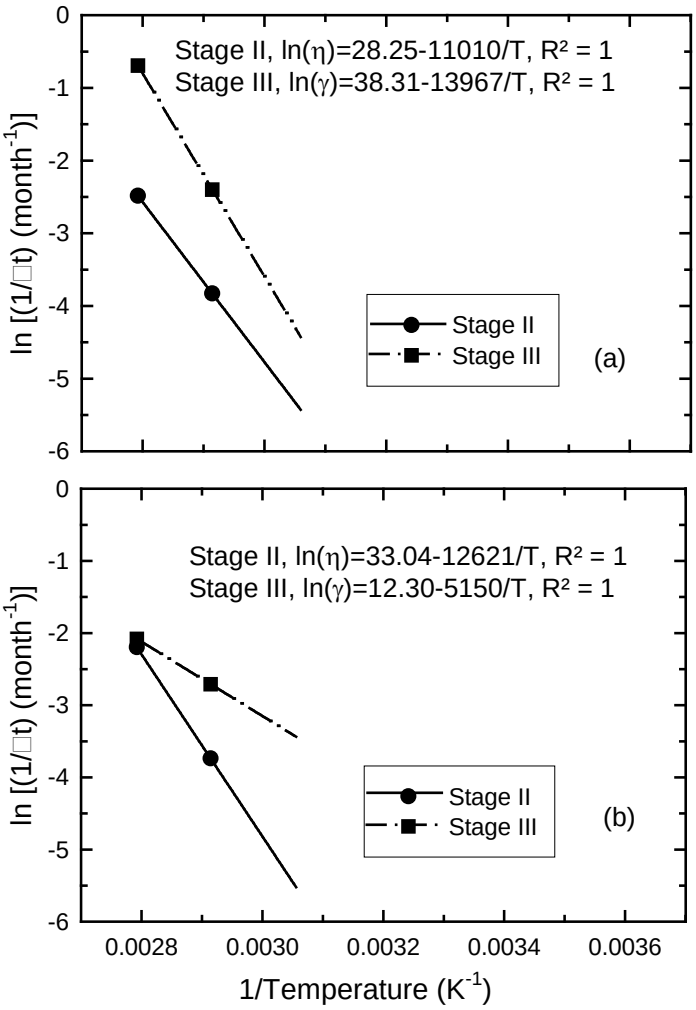

Figure 15. Arrhenius plot for Stage II and Stage III in water based on tensile break: (a) elongation and (b) strength.